Analysis of experimental data on neutron decay for the possibility of the existence of the right vector boson W_R

A. P. Serebrov,* O. M. Zherebtsov, A. K. Fomin, R. M. Samoilov, and N. S. Budanov
NRC "Kurchatov Institute" Petersburg Institute of Nuclear Physics, 188300, Gatchina, Russia

(Received 15 May 2025; accepted 7 November 2025; published 3 December 2025)

The analysis of the latest most accurate experimental data on neutron decay for the possibility of the existence of the right vector boson W_R is carried out. As a result of the analysis within the framework of the left-right symmetric model, it was found that there is an indication of the existence of the right vector boson W_R with a mass of $M_{W_R} = 304^{+24}_{-20}$ GeV, and a mixing angle with W_L: $\zeta = -0.039 \pm 0.014$. It is shown that this result does not contradict the experiments at colliders to search for a hypothetical vector boson. In addition, it is shown that it is possible to describe the effects of CP violation in decays of neutral K-mesons and D-mesons using the parameters of the extended left-right symmetric model obtained from neutron decay, i.e., squared masses of the left and right bosons ratio and the mixing angle. The formation of baryon-lepton asymmetry of the Universe is considered within the framework of the left-right model of weak interaction with CP violation.

DOI: 10.1103/fl44-1b8b

I. INTRODUCTION

There is a hypothesis that sterile neutrinos are actually righthanded neutrinos [1,2]. This hypothesis is quite appropriate, for example, it is discussed in connection with the possibility of explaining dark matter by righthanded neutrinos. However, this idea requires experimental justification. Righthanded neutrinos can appear together with right vector bosons: $W_R^{\pm}$, Z_R. In this regard, the analysis of experimental data on neutron decay on the possibility of the existence of a right vector boson W_R was carried out.

Theoretical models with the introduction of right vector bosons have been well known [3–6] since the late 1970s. The most detailed analysis of neutron decay is presented in [7], where aspects of the possible contribution of right currents are also considered. Before analyzing the current experimental situation in neutron decay for the possible presence of right currents, we present a review that illustrated the increase in measurement accuracy and shows trends in the measured values for the neutron lifetime and decay asymmetries.

II. A REVIEW ILLUSTRATING THE INCREASE IN MEASUREMENT ACCURACY

The results of the neutron lifetime measurements, electron and neutrino asymmetries of neutron decay are presented in Figs. 1–4. It can be seen that significant progress has been made in the accuracy of neutron lifetime measurements over the past 25 years. In 2005, a revolutionary refinement of the neutron lifetime occurred thanks to the work [8]—the measurement of the neutron lifetime with a gravitational trap of ultracold neutrons. This result was later confirmed by measurements with a magnetic Ultra Cold Neutrons (UCN) trap at Petersburg Nuclear Physics Institute (PNPI) [9,10] in 2009 and finally, with even greater accuracy, by measurements with a magnetic UCN trap at Los Alamos National Laboratory (LANL) in 2018 [11] and in 2021 [12].

Finally, in December 2024, the result of a new beam experiment with electron detection instead of proton detection appeared, which confirmed the neutron lifetime measured with UCN [15].

Trends in neutron decay electron asymmetry measurements are shown in Fig. 2. In decay electron asymmetry measurements, significant changes in accuracy occurred at the PERKEO II [19] and PERKEO III [20,21]. The accuracy of measurements of decay asymmetry first increased by 3 times and then by another 2.5 times, and ultimately amounted to 0.17%. At the same time, the absolute value of the electron decay asymmetry increased by 2%.

Finally, and particularly important for our analysis of right currents, we must use the results of measurements of the neutrino asymmetry of neutron decay, where the measurement accuracy was significantly increased in 1998 by the experiment [22]. The result was later confirmed by the experiment [23] with the same accuracy. As a result, the value of the neutrino asymmetry presented in PDG [16] was determined.

Significant progress in the measurements of electron-neutrino asymmetries of neutron decay (a) has been

*Contact author: serebrov_ap@pnpi.nrcki.ru

Published by the American Physical Society under the terms of the Creative Commons Attribution 4.0 International license. Further distribution of this work must maintain attribution to the author(s) and the published article's title, journal citation, and DOI. Funded by SCOAP³.

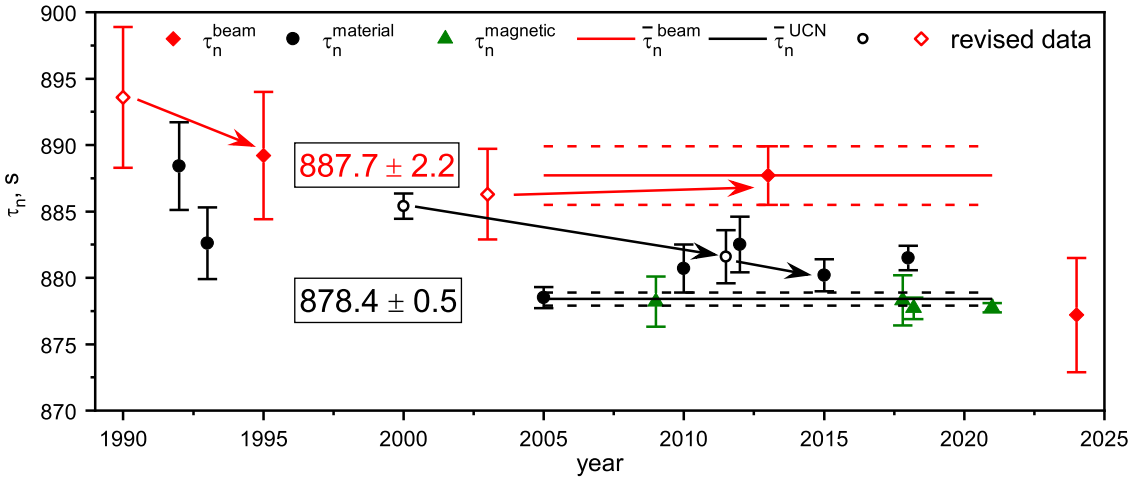


FIG. 1. Data of experimental results for the neutron lifetime, starting from 1990 from [13], discrepancy of data in 2005 [8] with data of 2000 [14], new results with magnetic trap (marked in green), which are decisive [9–12]. New beam experiment [15].

achieved in recent years in the experiment [24]. The experimental results of electron-neutrino asymmetries of neutron decay (a) and the averaged result from PDG are presented in Fig. 4.

In the following analysis, we will use the most precise result $a = -0.10402(82)$ from [18].

In addition, for further analysis, the unitarity condition of the Cabibbo-Kobayashi-Maskawa (CKM) matrix [25] and the data of experiments with Fermi superallowed nuclear $0^+ - 0^+$ transitions [26]. A graphical analysis of the listed measurement results is presented in Fig. 5.

Within the V-A theory of weak interaction, all three methods of V_{ud} determination (from neutron decay, from experiments with Fermi superallowed nuclear $0^+ - 0^+$ transitions and from the unitarity of the CKM matrix) must coincide. The results of determination V_{ud} from neutron decay are determined by the accuracy of measuring the neutron lifetime 877.75 ± 0.35 s [12] (blue area in Fig. 6) and the accuracy of measuring the ratio of the axial and vector constants from the electron asymmetry of neutron decay—$\lambda = -1.2757(5)$ [21] (green area in Fig. 6). The intersection of the data for the neutron lifetime and the value of the ratio of the axial and vector constants of the weak interaction λ from the electron asymmetry of neutron decay A gives the value $V_{ud}^n = 0.97477(37)$ [27].

From the unitarity of the CKM matrix, using the value $V_{us} = 0.2243(8)$ [16] and $|V_{ub}|^2 = 1.710^{-5}$ [16] can be calculated $V_{ud}^{\text{unit}} = \sqrt{1 - V_{us}^2 - V_{ub}^2} = 0.97452(18)$. This value agrees within the error limits with the value from neutron decay V_{ud}^n, however, the matrix element V_{ud}^{00} from $0^+ - 0^+$ transitions is noticeably different. $V_{ud}^{00} = 0.97373(32)$ [26] (Fig. 6). The difference V_{ud} between the matching values V_{ud}^n and the value V_{ud}^{00} from $0^+ - 0^+$ the transitions is 2.6σ. It is important to note that in [26] a

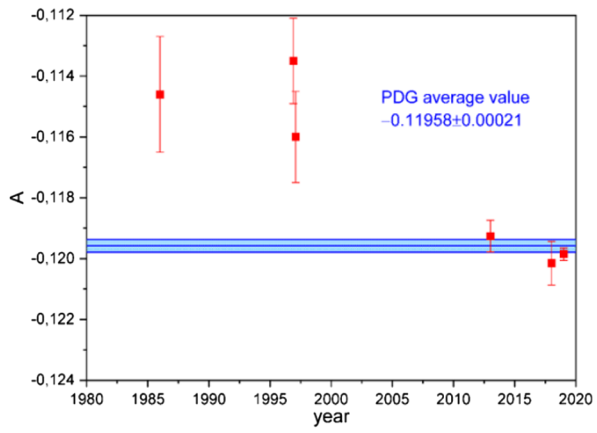


FIG. 2. Measurements of the electron asymmetry of neutron decay (A) and the averaged result from PDG [16].

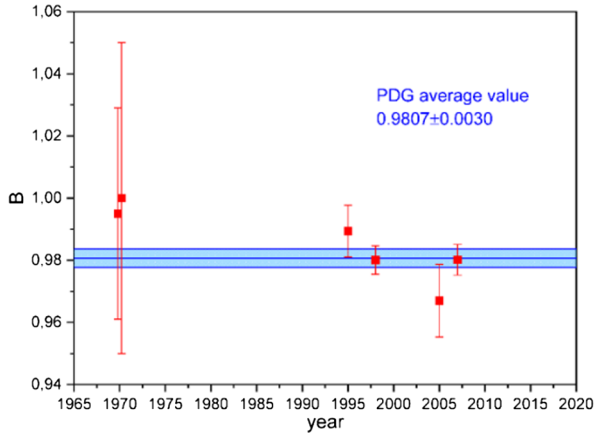


FIG. 3. Experimental results of neutrino asymmetry of neutron decay (B) and averaged result from PDG.

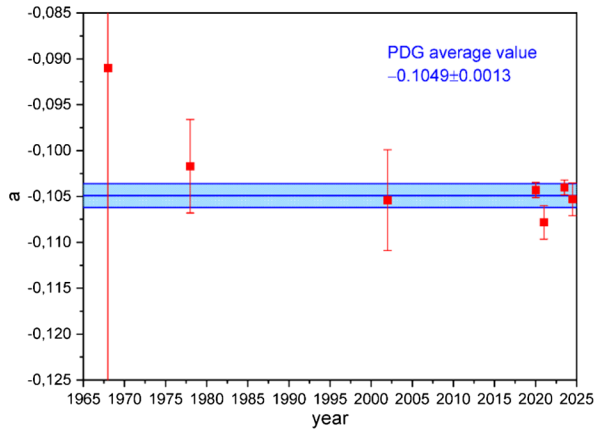


FIG. 4. The experimental results for the electron-neutrino asymmetry in neutron decay a, including the results from the aCORN [17] and aSPECT [18] experiments, as well as the averaged result from PDG [16].

violation of unitarity is equal to 2.4σ, which is also discussed in [28].

Figure 7 shows a comparison of the experimental neutrino decay asymmetry values $B = 0.9807(30)$ [16] and the calculated asymmetry within the SM framework depending on λ. In this case, there is also a discrepancy between the experimental value of the neutrino asymmetry and the SM prediction. The difference in the values of these quantities is 2.1σ. The best experimental test is to measure the neutrino asymmetry of neutron decay. Note that there are practically no radiative corrections for the neutrino asymmetry, internal radiative corrections occur at a level of about 10^{-5} [29], therefore, measuring neutrino asymmetry is the purest test for right currents. It was for this purpose that the works [22,23,30] were carried out.

At the same time, in [31] was shown that, consideration of the emission of real photons leads to a change in the proton recoil momentum, which is used to determine the

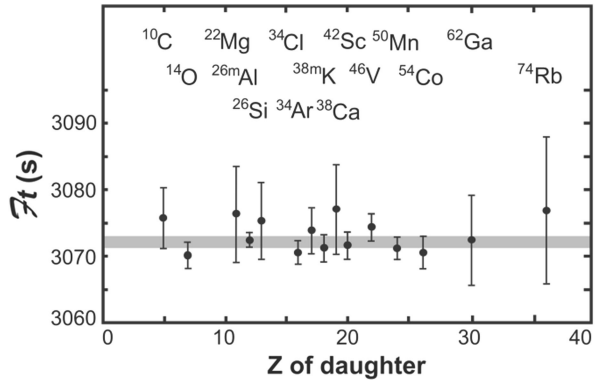


FIG. 5. Results of measuring the quantity $F\tau$ in experiments with Fermi superallowed nuclear $0^+ - 0^+$ transitions from work [26].

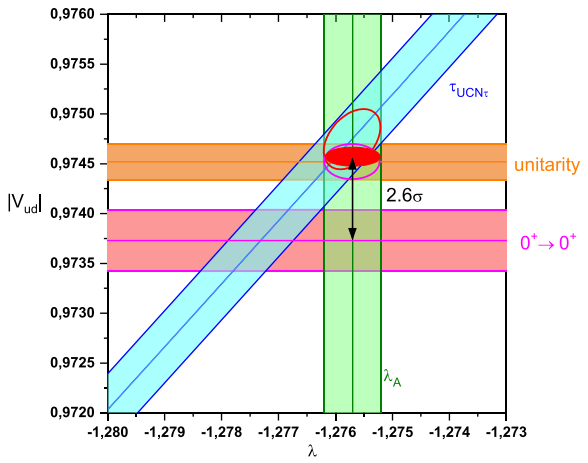


FIG. 6. Dependence of the matrix element of quark mixing V_{ud} on λ, calculated using the SM formulas from neutron decay, from experiments with Fermi superallowed nuclear $0^+ - 0^+$ transitions and from the unitarity of the CKM matrix, using measurements V_{us} [16].

antineutrino emission angle when processing experimental data. The magnitude of such a correction for the coefficient B is on the order of 0.1%. If such a correction is introduced to the value of B from [16], this will reduce the discrepancy between the experimentally measured value and the theoretical value from 2.1σ to 1.8σ, but will not eliminate it completely.

Finally, the most precise measurements of the electron-neutrino asymmetry (a) allow for an independent calculation of the λ_a value. However, it turns out that $\lambda_a = -1.2686 \pm 0.0025$, as reported in reference [18], differs from $\lambda_{A/\tau} = -1.2754 \pm 0.0013$ by 2.5σ. This discrepancy is illustrated in Fig. 8 from [17].

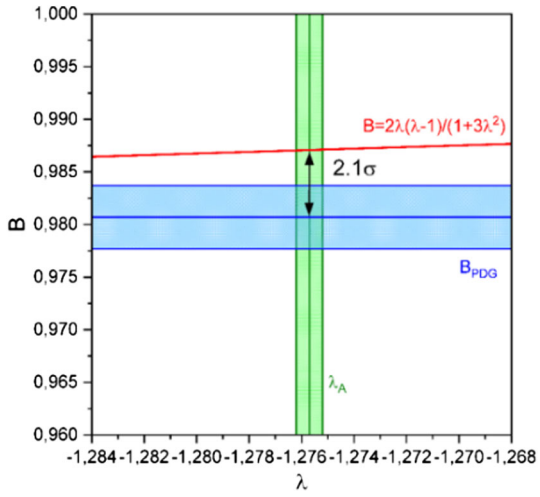


FIG. 7. Comparison of the experimental neutrino asymmetry of neutron decay and that calculated within the SM framework as a function of the ratio of the axial and vector constants of weak interaction λ.

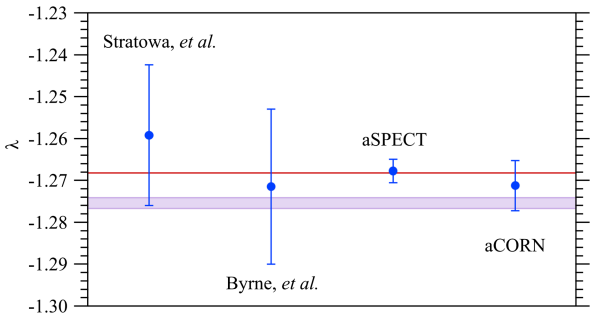


FIG. 8. The main results for the determination of λ from experiments measuring the coefficient a. The horizontal line represents the weighted average $\lambda = -1.2686 \pm 0.0025$. The shaded band shows the value $\lambda = -1.2754 \pm 0.0013$ from PDG 2022, which was obtained from measurements of the parameters A and τ.

From the presented picture of experimental data it follows that significant progress has been achieved in the accuracy of measurements and at the same time deviations in the interpretation of data within the framework of the V-A theory of weak interaction has been discovered. In this connection it is advisable to conduct an analysis taking into account the possible influence of right currents.

III. MANIFEST LEFT-RIGHT SYMMETRIC MODEL OF MIXING LEFT AND RIGHT VECTOR BOSONS

The analysis of the observed discrepancy can be done within the framework of the model taking into account the right currents. In the simplest left-right symmetric model [3–5], the mixing of left and right vector bosons is considered, and for flavor states W_L, W_R and mass states W_1, W_2 we can write [5]

$$\begin{aligned} W_L &= W_1 \cos\zeta + W_2 \sin\zeta \\ W_R &= e^{i\omega}(-W_1 \sin\zeta + W_2 \cos\zeta) \end{aligned} \tag{3.1}$$

where $\zeta =$ angle of mixing of current states W_L and W_R, and $\delta =$ ratio of the squares of the masses of states W_1 and W_2.

ω-CP-violating phase. Complete CP violation at $\omega = \pi/2$ and absence of CP-violation at $\omega = 0$.

However, it turned out that the use of the left-right manifest model does not resolve the unitarity problem for $0^+ \to 0^+$ transitions. Therefore, we propose considering an extended version of the left-right model of weak interaction with CP violation, which is introduced differently than in the manifest model. In this new version of the left-right model, we treat W^- and W^+ as particle and antiparticle, respectively. Consequently, the mixing matrices for negatively and positively charged bosons are Hermitian conjugates of each other, which explains the sign changes for the sines. We introduce CP violation between particles and antiparticles through W^- and W^+, which define the nature of the weak interaction and serve as particles and antiparticles. Thus, we should write

$$\begin{pmatrix} W_L^{\pm} \\ W_R^{\pm} \end{pmatrix} = \begin{pmatrix} \cos\zeta & \mp\sin\zeta \\ \pm\sin\zeta & \cos\zeta \end{pmatrix} \begin{pmatrix} W_1^{\pm} \\ W_2^{\pm} \end{pmatrix} \tag{3.2}$$

In the scheme of mixing left and right charged vector bosons (W^-) the plus sign is chosen for particles, and (W^+) the minus sign is chosen for antiparticles at the sine in the top row.

It should be noted that in the scheme (3.2) we are considering there is an important difference compared to the commonly used scheme (3.1), which does not take into account the different sign of mixing for particles and antiparticles. In this scheme, we essentially introduce a difference in the coupling constants of (W^-) and (W^+), i.e., particles and antiparticles, which will lead to CP violation.

We have examined the unitarity problem for $0^+ \to 0^+$ transitions within the framework of the left-right manifest model and the extended left-right model. The results of the analysis are presented in Fig. 9.

As can be seen, it is not possible to reconcile the values of V_{ud}^{00} and V_{ud}^{n} with V_{ud}^{unit} in either case. However, the case of the extended Standard Model is of interest due to the symmetric placement of V_{ud}^{00} and V_{ud}^{n} around V_{ud}^{unit}. It is important to note that the value V_{ud}^{00} is determined by the decay of W^+, while the value V_{ud}^{n} is determined by the decay of W^-. This asymmetry between particles and antiparticles arises due to CP violation. In the extended left-right model, this asymmetry originates from the different signs of the mixing of the right-handed vector boson $W_R^{\pm}$ with the left-handed vector boson $W_L^{\pm}$.

In the presented scheme, transitions are allowed only between W_1^- and W_2^-, as well as W_1^+ and W_2^+. All other transitions are prohibited due to the violation of the law of conservation of electric charge.

In this model, we consider left bosons. W_1^- and W_1^+ as particles and antiparticles, respectively. Moreover, W_1^- has *a negative charge* in accordance with the charge of the electron, appearing after the decay, and has *a negative (left) parity* in accordance with the negative (left) chirality of the antineutrino. For W_1^+ in accordance with the charge and spatial conjugation (CP) we have *a positive charge* in accordance with the charge of the positron, appearing after the decay, and have *a positive (right) parity* in accordance with the positive (right) chirality of the neutrino. Thus, we introduce into consideration the concept of P-parity for W_1^- and W_1^+, identifying it with the P-parity of the neutrino during decay.

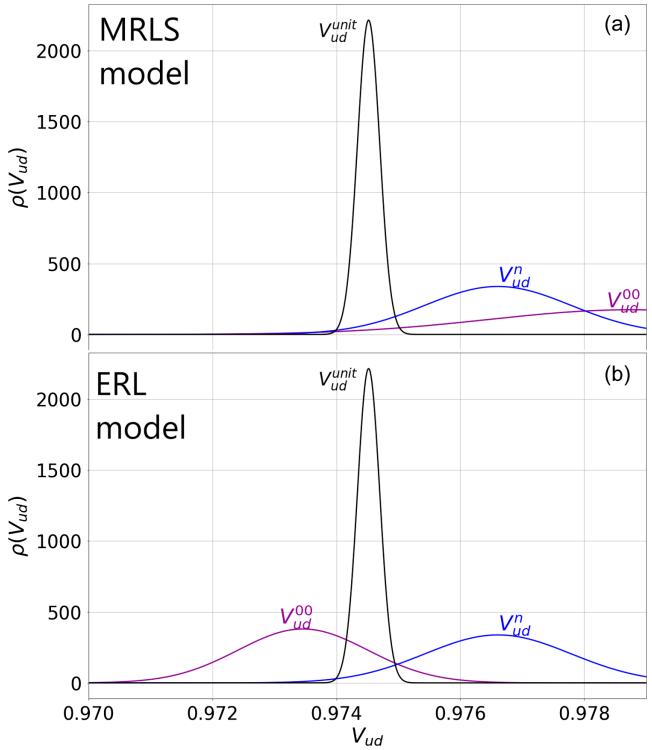


FIG. 9. Comparison of the values of V_{ud} obtained from data on neutron decay, superallowed Fermi transitions, and the requirement of CKM matrix unitarity within the framework of two models. In all plots, $V_{ud}^{\text{unit}} = 0.97452(18)$, derived from the unitarity condition and experimental values $V_{us} = 0.2243(8)$ and $|V_{ub}|^2 = 1.7 \times 10^{-5}$. (a) The left-right manifest model as presented in work [5]. (b) The extended left-right model, introduced in this work.

Then the right vector bosons W_2^- and W_2^+ have opposite parity to the left vector bosons, but are antiparticles, so the charge parity changes. In accordance with charge and spatial conjugation (CP), we have

$$\begin{aligned}
&W_1^-\text{—left particle } (C=-1, P=-1), CP=+1\\
&W_1^+\text{—left antiparticle } (C=+1, P=+1), CP=+1\\
&W_2^-\text{—right particle } (C=-1, P=-1), CP=+1\\
&W_2^+\text{—right antiparticle } (C=+1, P=+1), CP=+1
\end{aligned} \tag{3.3}$$

The rules (3.3) described above are shown in Fig. 10. Note that in the final state, in the case of W_1^- and W_2^- the light antineutrino and heavy antineutrino are mixed, and in the case of W_1^+ and, W_2^+ the light neutrino and heavy neutrino are mixed.

W_1^- and W_1^+ have positive CP parity.

W_2^- and W_2^+ have positive CP parity.

Thus, CP parity is conserved for W_1 and W_2, although these are particles of different masses. This is the most

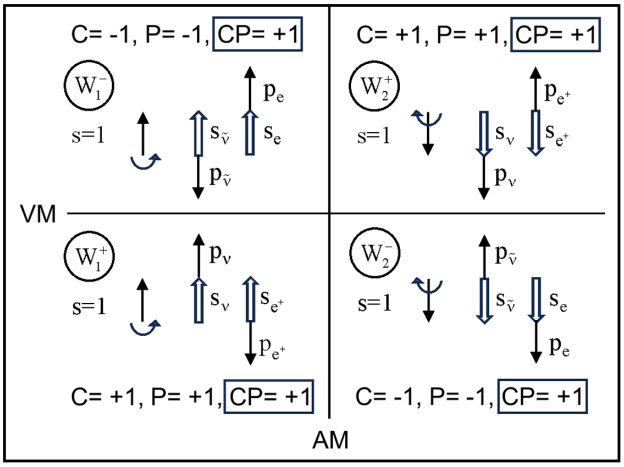


FIG. 10. Mixing diagram between W_1^- and W_2^-, as well as W_1^+ and W_2^+. VM is a mirror of vectors, AM is a mirror of axial vectors.

important feature of the left-right scheme, in which there is a mixing of a light antineutrino and a heavy antineutrino, as well as mixing of a light neutrino and a heavy neutrino, i.e., neutrinos of the same chirality.

The weak interaction Hamiltonian in the case where only vector and axial currents (V-A) are present can be represented in the well-known general form, for example [7].

$$\begin{aligned}
H_{V,A}^N = {}& \bar e\gamma_\mu(C_V + C_V'\gamma_5)\nu \cdot \bar p\gamma_\mu n\\
&- \bar e\gamma_\mu\gamma_5(C_A + C_A'\gamma_5)\nu \cdot \bar p\gamma_\mu\gamma_5 n + \text{H.c.}
\end{aligned} \tag{3.4}$$

In the presence of right currents with mixing parameters $\delta = m_1^2/m_2^2$, where m_1 is the mass of the light W_1 and m_2 is the mass of the heavy W_2.

The coefficients C_V, C_V' and C_A, C_A' within the framework of the simplest manifest left-right symmetric model: $g_R = g_L$, $V_{ud}^R = V_{ud}^L$, $\omega = 0$ are given by the following expressions [7].

$$\begin{aligned}
C_V &= g_V\frac{G_F V_{ud}}{\sqrt{2}}(1-2\zeta+\delta), \quad C_V' = g_V\frac{G_F V_{ud}}{\sqrt{2}}(1-\delta)\\
C_A &= g_A\frac{G_F V_{ud}}{\sqrt{2}}(1+2\zeta+\delta), \quad C_A' = g_A\frac{G_F V_{ud}}{\sqrt{2}}(1-\delta)
\end{aligned} \tag{3.5}$$

According to the general formula from [7], in the absence of scalar and tensor contributions, the probability of transition (neutron decay) is proportional to the product of the phase space and the lifetime to the power of -1, i.e., a value $(f\tau)_n^{-1}$ equal to

$$
\begin{aligned}
(f\tau)_n^{-1} &= |M_F|^2(|C_V|^2 + |C'_V|^2) \\
&\quad + |M_{GT}|^2(|C_A|^2 + |C'_A|^2) \\
|C_V|^2 + |C'_V|^2 &= |g_V G_F V_{ud}|^2(1-\zeta)^2 \\
&\quad \times (1 + ((\delta-\zeta)/(1-\zeta))^2). \\
|C_A|^2 + |C'_A|^2 &= |g_A G_F V_{ud}|^2(1+\zeta)^2 \\
&\quad \times (1 + ((\delta+\zeta)/(1+\zeta))^2).
\end{aligned} \tag{3.6}
$$

If we are only interested in quadratic contributions, we can write a simplified expression

$$
|C_V|^2 + |C'_V|^2 = |g_V G_F V_{ud}|^2(1-\zeta)^2(1+(\delta-\zeta)^2) \tag{3.7}
$$

$$
|C_A|^2 + |C'_A|^2 = |g_A G_F V_{ud}|^2(1+\zeta)^2(1+(\delta+\zeta)^2) \tag{3.8}
$$

For $0^+ \to 0^+$ transitions that occur with the decay of the mixed state W_1^+ and W_2^+ we must choose the appropriate sign of the mixing angle. This means that in formula (3.7) for $0^+ \to 0^+$ transitions we must change the sign in front of ζ.

From the experiment we can extract only the matrix elements taking into account the mixing of vector bosons, i.e., $\tilde{V}_{ui}$, where $(i = d, s, b)$. This means that we must renormalize the matrix elements for the model-independent approach considered in the work of P. Herczeg [6]. In the linear approximation this means that for $0^+ \to 0^+$ transitions, i.e., for W^+

$$
\tilde{V}_{ud}^{+} = V_{ud}^{+}(1+\zeta) = V_{ud}^{+(V)} \equiv V_{ud}^{00(V)},
$$

and for the decay of a neutron, i.e., for W^-

$$
\begin{aligned}
\tilde{V}_{ud}^{-} &= V_{ud}^{-}(1-\zeta) = V_{ud}^{-(V-A)} \equiv V_{ud}^{00(V-A)}. \\
(f\tau)_{00}^{-1} &= |M_F|^2(|C_V|^2 + |C'_V|^2) \\
&= |M_F|^2 |g_V G_F V_{ud}|^2(1+\zeta)^2(1+(\delta+\zeta)^2)
\end{aligned} \tag{3.9}
$$

Thus, the matrix element within the left-right model, extracted from $0^+ \to 0^+$ the transitions (V_{ud}^{00LR}) equals

$$
V_{ud}^{00LR} \simeq V_{ud}^{00(V)} \sqrt{[1+(\delta+\zeta)^2]} \tag{3.10}
$$

However, it is necessary to additionally take into account the effect of renormalization of the decay probability due to the additional decay channel through W_2^+. The total decay probability considering the mixing angle is proportional $1+\zeta^2$, so for renormalization it is necessary to introduce a factor $(1+\zeta^2)^{-1}$.

$$
V_{ud}^{00LR} = V_{ud}^{00(V)} \sqrt{\frac{[1+(\delta+\zeta)^2]}{1+\zeta^2}} \tag{3.11}
$$

Note that V_{ud}^{00LR} this is a matrix element extracted from the process of antiparticle decay W_1^+. $V_{ud}^{00LR} \equiv V_{ud}^{LR}(W^+)$

For the decay of a neutron

$$
\begin{aligned}
(f\tau)_n^{-1} &= |M_F|^2(|C_V|^2 + |C'_V|^2) + |M_{GT}|^2(|C_A|^2 + |C'_A|^2) \\
&= |M_F|^2 |g_V G_F V_{ud}|^2(1-\zeta)^2(1+(\delta-\zeta)^2) \\
&\quad + |M_{GT}|^2 |g_A G_F V_{ud}|^2(1+\zeta)^2(1+(\delta+\zeta)^2),
\end{aligned} \tag{3.12}
$$

where $|M_F|^2 = 1$, $|M_{GT}|^2 = 3$

We take out $2|M_F|^2|g_V G_F V_{ud}|^2(1-\zeta)^2$ the common factor and for the neutron we get

$$
\begin{aligned}
(f\tau)_n^{-1} &= |M_F|^2 |g_V G_F V_{ud}|^2(1-\zeta)^2 \\
&\quad \times \left\{ (1+(\delta-\zeta)^2) + \frac{|M_{GT}|^2|g_A|^2}{|M_F|^2|g_V|^2} \frac{(1+\zeta)^2}{(1-\zeta)^2} \right. \\
&\quad \left. \times (1+(\delta+\zeta)^2) \right\}
\end{aligned} \tag{3.13}
$$

where, as a first approximation $\widetilde{V_{ud}^{n}}^2 = V_{ud}^2(1-\zeta)^2$,

$$
\begin{aligned}
\tilde{V}_{ud}^{-} &= V_{ud}^{-}(1-\zeta) = V_{ud}^{-(V-A)} \\
\tilde{\lambda}_n^2 &\equiv \frac{|g_A|^2}{|g_V|^2} \frac{(1+\zeta)^2}{(1-\zeta)^2},
\end{aligned}
$$

which corresponds (taking into account the notations) to the definition λ in formula (29) from the work of P. Herczeg [6]. $\frac{|M_{GT}|^2}{|M_F|^2} = 3$, $\tilde{\lambda}_n^2 \equiv \lambda_{n,V-A}^2$.

Taking into account the quadratic terms, including the effect of renormalization of the decay probability due to the additional decay channel via W_2^-

$$
\begin{aligned}
&(f\tau)_n^{-1} \\
&= G_F^2 |g_V|^2 (V_{ud}^{n(V-A)})^2 (1+3\lambda_{n,V-A}^2) \\
&\quad \times (1+\zeta^2)^{-1} \left\{ 1 + (\delta^2+\zeta^2) + 2\frac{(3\lambda_{n,V-A}^2 - 1)}{(3\lambda_{n,V-A}^2 + 1)} \delta\zeta \right\}
\end{aligned} \tag{3.14}
$$

Let us introduce into consideration the matrix element $V_{ud}^{n,LR}$, defined according to the formula

$$
G_F^2 |g_V|^2 (V_{ud}^{n,LR})^2 (1+3\lambda_{\mathrm{exp},LR}^2) = (f\tau)_n^{-1}, \tag{3.15}
$$

$\lambda_{\mathrm{exp},LR}$–a value determined from the experiment using the formulas of the left-right model, taking into account the results of measurements: the neutron lifetime τ and decay asymmetries: a, B, and A. The relations for τ, a, B, and A within the left-right model will be presented in the next section.

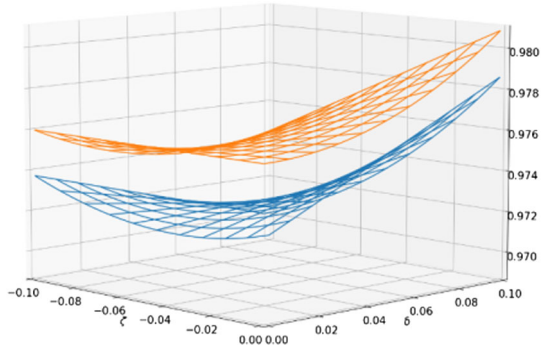


FIG. 11. Values of axial-vector $V_{ud}^{LR}(W^-)$ and vector $V_{ud}^{LR}(W^+)$ on the plane δ and ζ calculated using formulas (3.11), (3.16).

Thus, the matrix element within the left-right model extracted from the decay of a neutron (V_{ud}^{nLR}) is

$$V_{ud}^{nLR} = V_{ud}^{n(V-A)} \times \sqrt{\frac{1+3\lambda_{n,V-A}^2}{1+3\lambda_{\exp,LR}^2}\frac{\left[1+(\delta^2+\zeta^2)+2\frac{(3\lambda_{n,V-A}^2-1)}{(3\lambda_{n,V-A}^2+1)}\delta\zeta\right]}{(1+\zeta^2)}} \tag{3.16}$$

Note that V_{ud}^{nLR} is a matrix element extracted from the decay process with particle W_1^-. $V_{ud}^{nLR} \equiv V_{ud}^{LR}(W^-)$.

Since the mixing angle has a different sign for particles and antiparticles, it is possible that the values of $V_{ud}^{LR}(W^-)$ and $V_{ud}^{LR}(W^+)$ may differ, in addition, these are vector and axial-vector transitions. The calculation carried out using formulas (3.11), (3.16) is presented in Fig. 11 and confirms this difference.

The calculation carried out using formulas (3.11) and (3.16) is presented in Fig. 9(b) and confirms this difference.

Thus, due to CP violation, a splitting of the values of V_{ud} for W^- and W^+ occurs.

We assume that the unitarity of the CKM within the left-right model should be satisfied for the mean value of the sum of squares vector $V_{ud}^{LR}(W^+)$ and axial-vector $V_{ud}^{LR}(W^-)$ matrix elements. According to the left-right model, we use different signs in the mixing matrix for W^- and W^+. As a result, we have got that the elements of the CKM matrix are split. However, the average value of V_{ud} is conserved because it represents the average probability.

$$(V_{ud}^{LR})^2 = \frac{1}{2}[V_{ud}^{LR}(W^+)^2 + V_{ud}^{LR}(W^-)^2] \tag{3.17}$$

Above, the notations $\tilde{V}_{ud}$ from the work of P. Herczeg [6] were used, which are identical to the notations presented below, and the values of these quantities have already been determined from the experiment [26,27].

$$\tilde{V}_{ud}^{n} \equiv V_{ud}^{n(V-A)} = 0.97477(37) \tag{3.18}$$

$$\tilde{V}_{ud}^{00} \equiv V_{ud}^{00(V-A)} = 0.97367(32) \tag{3.19}$$

IV. ANALYSIS OF NEUTRON DECAY WITHIN THE LEFT-RIGHT MODEL

Experimental studies of neutron decay provide extremely important information for testing the Standard Model of particle physics (SM). Within the SM, neutron decay is described by the V-A version of the weak interaction theory. The probability of decay is determined by a number of parameters extracted from the experiment. The general formula for describing neutron decay within the V-A version of the weak interaction theory can be represented by the following expression.

$$\frac{d^3\Gamma}{dE_e d\Omega_e d\Omega_\nu} = \frac{1}{2(2\pi)^5} G_F^2 {V_{ud}}^2 (1+3\lambda^2) p_e E_e (E_0 - E_e)^2 \times \left[1 + a\frac{\vec{p}_e\cdot\vec{p}_\nu}{E_e E_\nu} + b\frac{m_e}{E_e} + \frac{\langle\vec{\sigma}_n\rangle}{\vec{\sigma}_n}\left(A\frac{\vec{p}_e}{E_e} + B\frac{\vec{p}_\nu}{E_\nu} + D\frac{\vec{p}_e\times\vec{p}_\nu}{E_e E_\nu}\right)\right] \tag{4.1}$$

The decay probability is proportional to the square of the coupling constant G_F with a fairly good accuracy obtained from the muon decay and is also proportional to the square of the matrix element V_{ud} of the CKM matrix. The matrix element is determined fairly accurately from the unitarity of the CKM matrix, given that the matrix elements V_{us} and V_{ub} are determined from the decay of strange and charmed mesons. The remaining parameters in this formula a, A, B, and D, as well as the neutron lifetime τ must be determined from experiment. The parameter λ, which is the ratio of the axial and vector weak coupling constants G_A/G_V, must be determined using the experimental values of a, A, B and τ, based on the V-A version of the weak interaction theory. The ratio G_A/G_V is renormalized by the strong interaction of quarks, and therefore differs from unity. For the V-A version of the theory, the Fierz term b is zero. In the following we will assume that there is no T violation, since $D = -1.2(2.0)10^{-4}$ [16].

For experimental results a, A, B, and τ within the framework of the V-A version of the theory, the following formulas can be written below.

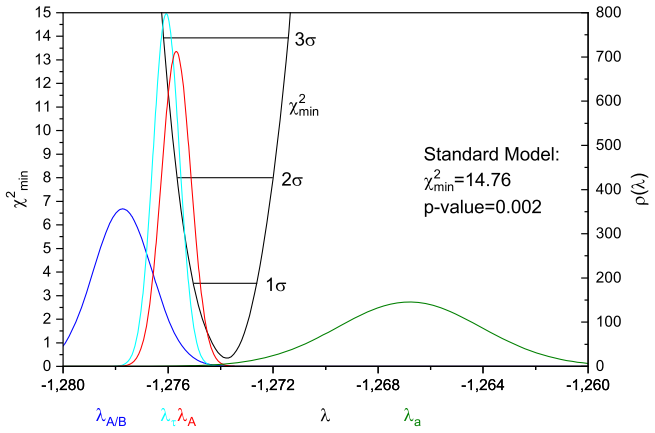


FIG. 12. Results of calculating the λ parameter value within the framework of the V-A theory of weak interaction.

$$\begin{aligned}\tau_{\text{exp}} &= \frac{4905.7}{V_{ud}^2(1+3\lambda^2)}\\ a_{\text{exp}} &= \frac{(1-\lambda^2)}{(1+3\lambda^2)}\\ A_{\text{exp}} &= -\frac{2\lambda(\lambda+1)}{1+3\lambda^2}\\ B_{\text{exp}} &= \frac{2\lambda(\lambda-1)}{1+3\lambda^2}\end{aligned} \tag{4.2}$$

And the experimental results

$$\begin{aligned}\tau_{\text{exp}} &= 877.75(35)\\ a_{\text{exp}} &= -0.10402(82)\\ A_{\text{exp}} &= -0.11958(21)\\ B_{\text{exp}} &= 0.9807(30)\\ V_{ud}^{\text{unit}} &= 0.97452(18)\end{aligned} \tag{4.3}$$

From the formulas for A_{exp} and B_{exp} it follows that

$$A_{\text{exp}}/B_{\text{exp}} = \frac{1+\lambda}{1-\lambda}.$$

For τ, we use the most precise value of the neutron lifetime from the PDG, although the latest refined result, $\tau = 877.82 \pm 0.22^{+0.20}_{-0.17}$ s, is presented in work [32]. The refined result does not affect the results of our analysis within the current level of precision.

Using these relations and experimental results, taking into account internal and external radiation corrections, it is possible to calculate the corresponding values of the parameter λ. The results of these calculations are presented in Fig. 12.

When calculating the value of λ (Fig. 12), the ratio of the coefficients A/B is used, so in this case the relative change in λ is an order of magnitude smaller than the relative change in the coefficient B. Thus, a relative change in B by $\mathcal{O}(10^{-3})$ leads to a relative change in λ of the order of 10^{-4}. This means that the value of $\lambda_{\text{opt}} = -1.2738 \pm 0.001$ used in the analysis for right-hand currents will not shift beyond its error limits when the value of B changes by a value of the order of 10^{-3}.

It can be seen that the proposed description within the V-A of theory turns out to be unsatisfactory. For the best fit using only the Standard Model $\chi^2 = 14.76$, p-value $= 0.002$. Thus, there is a deviation from the SM by more than 3σ. In connection with the current situation in determining the parameter, λ we decided to conduct an analysis of the possible contribution of right currents in weak interaction, i.e., for the presence of a right vector boson W_R. The formulas describing the possible mixing W_L and W_R are presented in detail in the review [7].

The task of the planned analysis of the possible contribution of right currents in the weak interaction is to find the best agreement between the experimental quantities τ_0, a_0, A_0, B_0 with a single set of parameters λ, δ and ζ. In this analysis, the value of $V_{ud}^n = 0.97477(37)$ [27], obtained from neutron decay, is used. This value differs from $V_{ud}^{\text{unit}} = \sqrt{1 - V_{us}^2 - V_{ub}^2} = 0.97452(18)$ by an amount that is negligible within the limits of experimental uncertainty.

$$\begin{aligned}\tau_{\text{exp}} \pm \Delta\tau_{\text{exp}} &= \frac{4905.7}{V_{ud}^2[1+(\delta-\zeta)^2+3\lambda^2(1+(\delta+\zeta)^2)]}\\ a_{\text{exp}} \pm \Delta a_{\text{exp}} &= \frac{(1-\lambda^2)[1+(\delta+\zeta)^2]-4\delta\zeta}{(1+3\lambda^2)[1+(\delta+\zeta)^2]-4\delta\zeta}\\ A_{\text{exp}} \pm \Delta A_{\text{exp}} &= -\frac{2\lambda[\lambda(1-(\delta+\zeta)^2)+(1-\delta^2+\zeta^2)]}{1+(\delta-\zeta)^2+3\lambda^2(1+(\delta+\zeta)^2)}\\ B_{\text{exp}} \pm \Delta B_{\text{exp}} &= \frac{2\lambda[\lambda(1-(\delta+\zeta)^2)-(1-\delta^2+\zeta^2)]}{1+(\delta-\zeta)^2+3\lambda^2(1+(\delta+\zeta)^2)}\end{aligned} \tag{4.4}$$

Within the framework of the manifest left-right symmetric model, the ratio of the difference between the experimental values and the values obtained by the standard V-A model to the value of the standard model can be represented (in an expansion in δ and ζ not higher than the second order) by the following expressions. In essence, this is a transition to a representation in relative deviations from the V-A theory.

Each of the equations gives three lines on the plane δ, ζ for positive, negative, and zero values of the measurement error. To obtain the optimal set of parameters λ, δ, and ζ calculations were carried out on the plane δ, ζ according to the formulas given above for different values of λ. As expected, for extreme values of $\lambda = -1.2677$ and $\lambda = -1.2784$ it is impossible to find a point on the plane δ, ζ, satisfying the above equations. This is the upper and lower graph in Fig. 13. However, it turned out to be possible to obtain the optimal set of parameters λ, δ, and ζ for the value

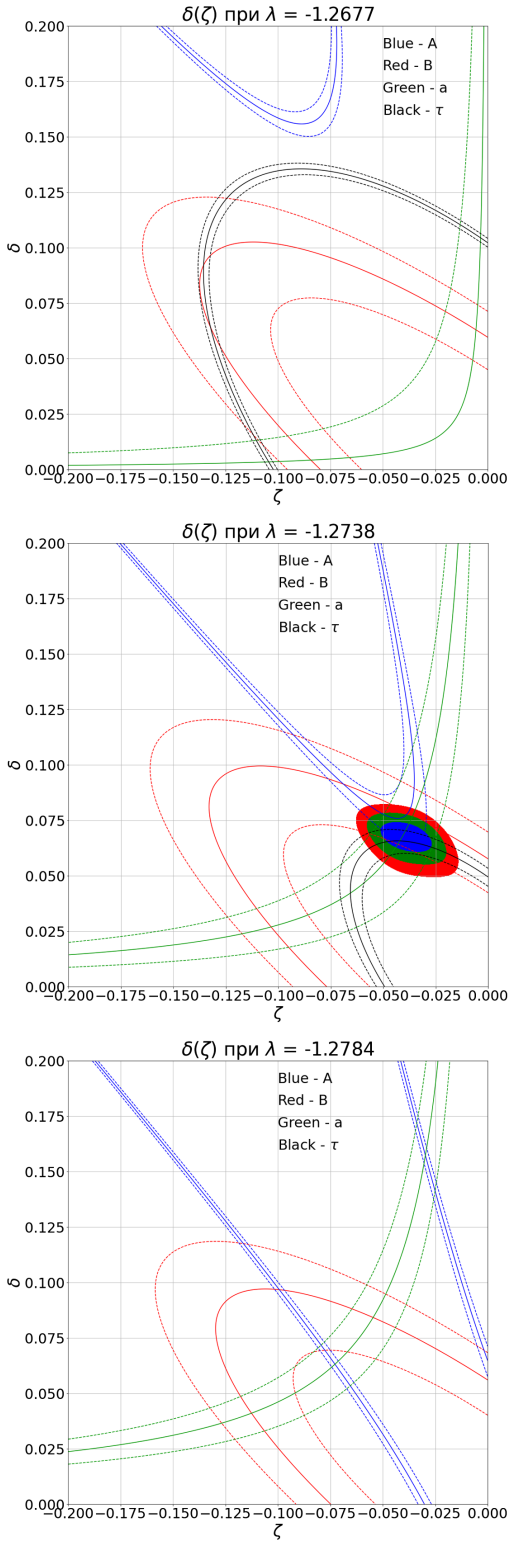


FIG. 13. Dependence of parameter δ on parameter ζ from equations (4.4) for the results of measuring quantities a, A, B and τ for different values of parameter λ. Upper and lower graphs for extreme values of $\lambda = -1.2677$ and $\lambda = -1.2784$, where it is impossible to find a point on the plane δ, ζ, satisfying the above equations. Middle graph for the optimal set of parameters λ, δ, and ζ for the value $\lambda_{\text{opt}} = -1.2738$.

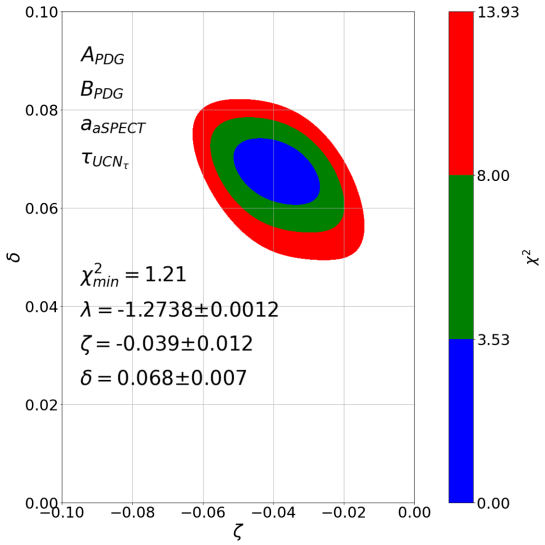


FIG. 14. Optimal values of the parameters λ, δ, and ζ, obtained by the method χ^2, using experimental data on neutron decay for a, A, B, and τ. $\chi^2_{\text{min}} = 1.21$.

of $\lambda_{\text{opt}} = -1.2738 \pm 0.0011$. This is the middle graph in Fig. 13.

$$\frac{\tau_{\text{exp}} \pm \Delta\tau_{\text{exp}} - \tau_{V-A}}{\tau_{V-A}} \simeq -\left[\delta^2 + \zeta^2 + 2\frac{(3\lambda^2-1)}{(3\lambda^2+1)}\delta\zeta\right] \quad (4.5)$$

$$\frac{a_{\text{exp}} \pm \Delta a_{\text{exp}} - a_{V-A}}{a_{V-A}} \simeq -\frac{16}{(1-\lambda^2)(1+3\lambda^2)}\delta\zeta \quad (4.6)$$

$$\frac{A_{\text{exp}} \pm \Delta A_{\text{exp}} - A_{V-A}}{A_{V-A}} \simeq -2\delta^2 - 2\delta\zeta\frac{[6\lambda^3+3\lambda^2-1]}{(\lambda+1)(1+3\lambda^2)} - 2\frac{\lambda}{\lambda+1}\zeta^2 \quad (4.7)$$

$$\frac{B_{\text{exp}} \pm \Delta B_{\text{exp}} - B_{V-A}}{B_{V-A}} \simeq -2\delta^2 - 2\delta\zeta\frac{[6\lambda^3-3\lambda^2+1]}{(\lambda-1)(1+3\lambda^2)} - 2\frac{\lambda}{\lambda-1}\zeta^2 \quad (4.8)$$

The calculations were carried out using formulas (4.4) and formulas (4.5)–(4.8), no significant difference was found.

A more accurate search for optimal values was made by the χ^2 method. The result of the analysis for λ_{opt} is shown in Fig. 12, and for δ_{opt} and ζ_{opt} the result is shown in Fig. 14. Due to this analysis, optimal values and the accuracy of their determination were determined. The analysis was made using the most accurate data from PDG 24 [16]. These are the neutron lifetime τ_n, electron asymmetry A, electron-neutrino correlation a.

Using the most accurate experimental data for a, τ and PDG data for A, B we obtained

$$\lambda_{\text{opt}} = -1.2738 \pm 0.0012.$$

As a result of the analysis within the framework of the manifest left-right symmetric model, using experimental data on neutron decay, an estimation of the mass of the right vector boson and the mixing angle was made: $M_{W_R} = 308^{+17}_{-15}$ GeV, $\zeta_{\text{opt}} = -0.039 \pm 0.012$.

In conclusion of this section, we present a correlation matrix for the parameters used in this analysis.

$$\begin{array}{cccc} & \zeta & \delta & \lambda \\ \zeta & 1 & -0.33 & -0.19 \\ \delta & -0.33 & 1 & 0.90 \\ \lambda & -0.19 & 0.90 & 1 \end{array} \tag{4.9}$$

V. CONSIDERATION OF THE ACCURACY OF CALCULATION OF RADIATION CORRECTIONS

Taking into account radiative corrections [33–35] plays an important role in precision experiments to measure the neutron lifetime—τ_n and the correlation coefficients of the neutron decay asymmetry—A and a to search for possible deviations from the predictions of the standard model [27,36,37]. In addition to radiative corrections, corrections for weak magnetism and the final mass of the nucleon (nonzero proton momentum) are also taken into account [38]. The neutron lifetime λ and the square of the modulus of the matrix element V_{ud} of the CKM matrix are related by the following expression [36].

$$\frac{1}{\tau_n} = \frac{G_F^2 {V_{ud}}^2}{2\pi^3} m_e^5 (1 + 3\lambda_n^2)(1 + \Delta_{\text{R}}) f, \tag{5.1}$$

where f is a factor related to the phase space [38] and takes into account the Fermi function, as well as the finite size and mass of the nucleus $f = 1.6887(1)$, Δ_{R} are the full radiative corrections. The expression for f can be found in [29]. The leading order of the full radiative corrections Δ_{R} is of the order of the fine structure constant α/π [34,35]. The so-called master formula is given in [27]

$${V_{ud}}^2 = \frac{4905.7(1.7)s}{\tau_n(1 + 3\lambda_n^2)}, \tag{5.2}$$

which is obtained from (5.1) with the value of radiative corrections Δ_{R} equal to 0.03947(32). There is also the new calculation result equal to 0.03983(27) from [39]. But it does not significantly change the results of our calculations, so we will use the old data for formula (5.2).

Radiative corrections in the form of a factor $(1 + \Delta_{\text{R}})$ can be represented as a product $(1 + \Delta_{\text{R}}) = (1 + \delta_R) \times (1 + \Delta_R^{\text{V}})$, where the contribution of the "outer" radiative correction δ_R was obtained by computing QED one-loop and bremsstrahlung diagrams, assuming that nucleons are pointlike, and the contribution of the "inner" radiative correction Δ_R^{V} that is sensitive to the details of SM electroweak theory and probes the hadronic structure of the nucleon [29]. In the [27] the master formula (5.2) was obtained from (5.1) with $\Delta_R^V = 0.02426(32)$. The new calculations of Δ_R^V based on data-driven dispersion relation can be found in [40–42] and based on lattice QCD in [43]. The average result is $\Delta_R^V = 0.02467(27)$ [39].

When measuring the correlation coefficient A in work [20], when fitting the experimental value of asymmetry, the necessary corrections are introduced for the final mass of nucleons (recoil protons) and weak magnetism, $g_V - g_A$ interference. In addition, the experimental value of asymmetry A takes into account radiation corrections, the value of which is of the order of 10^{-3} and the error is 10^{-4}.

When measuring the correlation coefficient a in [24], the proton energy spectrum was fitted using formulas from [44], which take into account radiation corrections of the order of the fine structure constant. Corrections for weak magnetism and Coulomb interaction were also taken into account.

In [29], expressions are given for the dependence of the coefficients a, A, and B on the electron energy with an accuracy of up to contributions of the order of 10^{-4}

It turns out that the influence of radiative corrections on the value of the coefficient B is smaller [27,45] than for the neutron lifetime. Table I shows a comparison of the error values of experiments on measuring the neutron lifetime and correlation coefficients in neutron beta decay with the

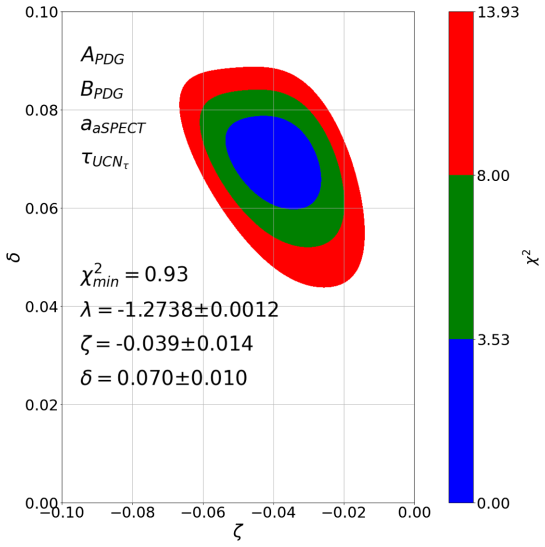


FIG. 15. Optimal values of the parameters δ and ζ obtained by the χ^2 method, using experimental data from neutron decay for a, A, B, and τ, taking into account an exaggerated level of precision for radiative corrections. The 1σ, 2σ, and 3σ regions are indicated. $\chi^2_{\text{min}} = 0.93$.

values of the corresponding radiative corrections and their uncertainties.

In the analysis conducted above, the precision of the radiative corrections was already taken into account through the error of 1.7 s in formula (5.2). However, to demonstrate their role, calculations can be carried out with level of precision that is higher than real, effectively taking these corrections into account a second time.

Below in Fig. 15 the results obtained for the PDG data are presented using experimental data on neutron decay for a, A, B, and τ taking into account accuracy of calculation of radiative corrections: $\lambda_{\text{opt}} = -1.2738 \pm 0.0012$, $\delta_{\text{opt}} = 0.070 \pm 0.010$ $M_{W_R} = 304^{+24}_{-20}$ GeV, $\zeta_{\text{opt}} = -0.039 \pm 0.014$.

As can be seen, the precision of determining the main parameters of the left-right model has remained practically unchanged, while the value of the minimal χ^2 has decreased because the errors were overstated.

Here we present a refined result for the parameters δ, ζ, which was previously presented in our work [46] with the following values $\mathrm{M_{W_R}} \approx 319^{+26}_{-20}$ GeV and the mixing angle with $\mathrm{W_L}$: $\zeta = -0.034 \pm 0.013$.

In conclusion, it is important to note that the analysis of the neutron decay was made within the framework of the conventional manifest left-right symmetric model considered in [3–5,7]. The extended version of the model with CP violation was not used, since we have so far considered the process involving only W^-. The extended version of the left-right model will be required when we consider transitions where the process $0^+ - 0^+$ occurs with W^+. Then it will be possible to compare the direct transition from the d-quark to the u-quark and the reverse transition from the u-quark to the d-quark and study the CP-violating asymmetry of the processes.

VI. CONSTRAINTS ON THE W' MASS OBTAINED IN COLLIDER EXPERIMENTS

Particle Data Group (PDG) has significantly stronger (> 6 TeV) constraints on the hypothetical vector boson W' obtained in accelerator experiments. It is necessary to distinguish between these constraints and it should be noted that they are in different subsections in PDG not by chance. The point is that constraints on the mass W_R can be obtained in the decay of neutrons and nuclei, these studies are a method of precision measurements alternative to research at colliders. This is a whole line of experiments that were discussed earlier, as well as a large number of theoretical works devoted to the analysis of these experimental data for possible deviations from the SM [3–6,28,47–53]. Our work complements this list and is focused mainly on the right currents, i.e., on the search for an admixture of the right vector boson.

TABLE I. The values of experimental errors and the corresponding radiative corrections with their uncertainties.

Size	Experimental error %	Correction %	Correction error %	Work
τ_n	0.040	3.947	0.032	[27]
A	0.176	−0.100	0.01	[20]
a	0.788	0.005	0.005	[55]
B	0.306	<0.1	<0.1	[31]

TABLE II. Coupling constants to quarks and leptons for left and right resonances.

For the left resonance	For the right resonance
$a_{ud}^{L^2} a_{l\nu}^{L^2} = (\cos^2\zeta + \delta \sin^2\zeta)^2$	$a_{ud}^{L^2} a_{l\nu}^{L^2} = (\sin^2\zeta + \delta \cos^2\zeta)^2$
$a_{ud}^{R^2} a_{l\nu}^{R^2} = (\sin^2\zeta + \delta \cos^2\zeta)^2$	$a_{ud}^{R^2} a_{l\nu}^{R^2} = (\sin^2\zeta + \delta \cos^2\zeta)^2$
$a_{ud}^{R^2} a_{l\nu}^{L^2} = (\delta-1)^2 \sin^2\zeta \cos^2\zeta e^{2i\omega}$	$a_{ud}^{R^2} a_{l\nu}^{L^2} = (\delta-1)^2 \sin^2\zeta \cos^2\zeta e^{2i\omega}$
$a_{ud}^{L^2} a_{l\nu}^{R^2} = (\delta-1)^2 \sin^2\zeta \cos^2\zeta e^{-2i\omega}$	$a_{ud}^{L^2} a_{l\nu}^{R^2} = (\delta-1)^2 \sin^2\zeta \cos^2\zeta e^{-2i\omega}$

The constraints on the hypothetical vector boson W' obtained in accelerator experiments mean that no resonances have been detected in the various decay modes up to energy of 6 TeV. at a cross section statistically available at the present time. Of course, the signals $e\nu$ from $e\mu$ the decay of the right vector boson are no different from the signals from the decay of the left vector boson, so the search is carried out with the background of similar events and with the background of other decay modes associated with the interaction of quarks and gluons.

Let us calculate the resonance production cross section of W_L and W_R bosons in high-energy proton collisions. We use formula (4) from [54] and the coupling constants to quarks and leptons from [5] to calculate the cross section. It is important to note that the left resonance is a process occurring with a small mixing angle ζ of the left vector boson W_L with the right vector boson W_R, and the right resonance is a process with a small mixing angle ζ of the right vector boson W_R with the left vector boson W_L. For this reason, the coupling constants in Table II for the left and right resonances are different.

Below is a modified formula for calculating the cross section from [54] and a table of coupling constants for the left and right resonance from [5].

$$\sigma(s) = \frac{\pi\alpha_W^2}{6} V_{ud}^2 \times \left[\frac{a_{ud}^{L^2} a_{l\nu}^{L^2} + a_{ud}^{R^2} a_{l\nu}^{R^2} + a_{ud}^{R^2} a_{l\nu}^{L^2} + a_{ud}^{L^2} a_{l\nu}^{R^2}}{(s - m_{W_L}^2)^2 + \gamma_{W_L}^2 m_{W_L}^2} + 2 a_{ud}^{L} a_{l\nu}^{L} \frac{(s - m_{W_L}^2)(s - M_{W_R}^2) + \gamma_{W_L}^2 \Gamma_{W_R}^2}{((s - m_{W_L}^2)^2 + \gamma_{W_L}^2 m_{W_L}^2)((s - M_{W_R}^2)^2 + \Gamma_{W_R}^2 M_{W_R}^2)} \right.$$
$$\left. \times \frac{a_{ud}^{L^2} a_{l\nu}^{L^2} + a_{ud}^{R^2} a_{l\nu}^{R^2} + a_{ud}^{R^2} a_{l\nu}^{L^2} + a_{ud}^{L^2} a_{l\nu}^{R^2}}{(s - M_{W_R}^2)^2 + \Gamma_{W_R}^2 M_{W_R}^2} \right]$$

$$\sigma(s) = \frac{\pi\alpha_W^2}{6} V_{ud}^2 \times \left[\frac{(\cos^2\zeta + \delta\sin^2\zeta)^2 + (\sin^2\zeta + \delta\cos^2\zeta)^2 + (\delta-1)^2\sin^2\zeta\cos^2\zeta e^{2i\omega} + (\delta-1)^2\sin^2\zeta\cos^2\zeta e^{-2i\omega}}{(s - m_{W_L}^2)^2 + \gamma_{W_L}^2 m_{W_L}^2} \right.$$
$$+ 2(\sin^2\zeta + \delta\cos^2\zeta) \frac{(s - m_{W_L}^2)(s - M_{W_R}^2) + \gamma_{W_L}^2 \Gamma_{W_R}^2}{((s - m_{W_L}^2)^2 + \gamma_{W_L}^2 m_{W_L}^2)((s - M_{W_R}^2)^2 + \Gamma_{W_R}^2 M_{W_R}^2)}$$
$$\left. + \frac{(\sin^2\zeta + \delta\cos^2\zeta)^2 + (\sin^2\zeta + \delta\cos^2\zeta)^2 + (\delta-1)^2\sin^2\zeta\cos^2\zeta e^{2i\omega} + (\delta-1)^2\sin^2\zeta\cos^2\zeta e^{-2i\omega}}{(s - M_{W_R}^2)^2 + \Gamma_{W_R}^2 M_{W_R}^2} \right]$$
$$= \frac{\pi\alpha_W^2}{6} V_{ud}^2 \times \left[\frac{(1+\delta^2) + 4\delta\sin^2\zeta\cos^2\zeta + (\delta-1)^2\sin^2\zeta\cos^2\zeta(e^{2i\omega} + e^{-2i\omega})}{(s - m_{W_L}^2)^2 + \gamma_{W_L}^2 m_{W_L}^2} \right.$$
$$+ 2(\sin^2\zeta + \delta\cos^2\zeta) \frac{(s - m_{W_L}^2)(s - M_{W_R}^2) + \gamma_{W_L}^2 \Gamma_{W_R}^2}{((s - m_{W_L}^2)^2 + \gamma_{W_L}^2 m_{W_L}^2)((s - M_{W_R}^2)^2 + \Gamma_{W_R}^2 M_{W_R}^2)}$$
$$\left. + \sin^2\zeta \frac{2\sin^2\zeta + 4\delta\cos^2\zeta + 2\frac{\cos^4\zeta}{\sin^2\zeta}\delta^2 + (\delta-1)^2\cos^2\zeta(e^{2i\omega} + e^{-2i\omega})}{(s - M_{W_R}^2)^2 + \Gamma_{W_R}^2 M_{W_R}^2} \right]. \tag{6.1}$$

Neglecting the small terms containing ζ and δ, we obtain a simplified expression without taking into account the interference effect. As can be seen, the resonance term for the right W_R contains the order suppression factor $\zeta^2 \approx 1.4 \times 10^{-3}$. This circumstance is the main reason why the resonance of the right W_R has not been detected in collider experiments.

$$\sigma(s) = \frac{\pi\alpha_W^2}{6} V_{ud}^2 \times \left[\begin{array}{c} \frac{1}{(s - m_{W_L}^2)^2 + \gamma_{W_L}^2 m_{W_L}^2} \\ + \sin^2\zeta \frac{2\sin^2\zeta + 4\delta\cos^2\zeta + 2\frac{\cos^4\zeta}{\sin^2\zeta}\delta^2 + (\delta-1)^2\cos^2\zeta(e^{2i\omega} + e^{-2i\omega})}{(s - M_{W_R}^2)^2 + \Gamma_{W_R}^2 M_{W_R}^2} \end{array} \right] \tag{6.2}$$

Let us calculate the cross section of resonance processes using the following values of the quantities included in this expression: $\alpha_W = \frac{1}{137}$, $V_{ud} = 0.97477$, $m_{W_L} = 80.385$ GeV, $\gamma_{W_L} = 2.141$ GeV, $M_{W_R} = 303.8$ GeV, $\Gamma_{W_R} = 11$ GeV, $\zeta = -0.039$, $\delta = 0.07$. Below in Fig. 16 we present the results of the calculation of the production cross section in relative units depending on the transverse mass at theoretical resonance widths: $\gamma_{W_L} = 2.141$ GeV, $\Gamma_{W_R} = 11$ GeV. The upper figure is without CP violation at $\omega = 0$, the lower figure is with CP violation at $\omega = \pi/2$. In Fig. 17 we present the results of the calculation taking into account the instrumental broadening in the experiment.

Fig. 17 presents the resonance widths are increased by 5 times to take into account the instrumental broadening in the experiment.

As can be seen, the reason why the right resonance W_R was not detected in the collider experiments is that the resonance term for the right W_R contains an order suppression factor $\zeta^2 \approx 1.4 \times 10^{-3}$ and that the instrumental broadening of the resonances significantly reduces the sensitivity of the experiment.

Below, in Fig. 18, we present a comparison of the calculation results with experimental data for the experiment at the Tevatron at Fermilab from publication [56] and for the ATLAS experiment [57] at CERN.

From this comparison, it follows that the expected effect from W_R with a mass of $M_{W_R} = 304$ GeV could not be detected in the experiment at the Tevatron at Fermilab, as this effect lies below the statistical significance of the experimental data.

Let us now consider the results of the ATLAS experiment [57], where the statistical precision is expected to be higher. The results of the ATLAS experiment [57] are shown in Fig. 19. Unfortunately, the region corresponding to the left resonance is not displayed on this plot, so the normalization was carried

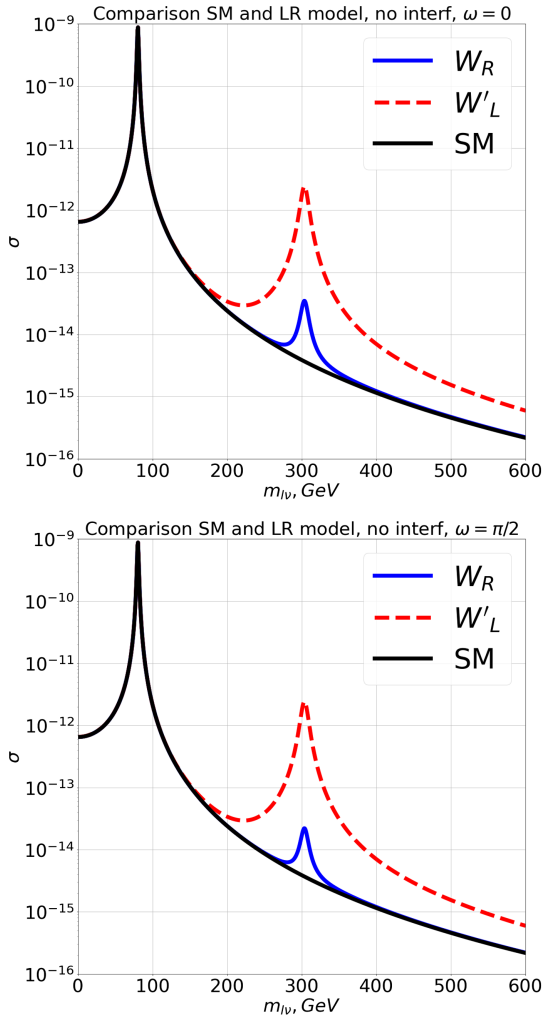


FIG. 16. Relative cross section of the W_R and W'_L production process at theoretical resonance widths: $\gamma_{W_L} = 2.141$ GeV, $\Gamma_{W_R} = 11$ GeV. The upper figure is for $\omega = 0$, the lower figure is for $\omega = \pi/2$.

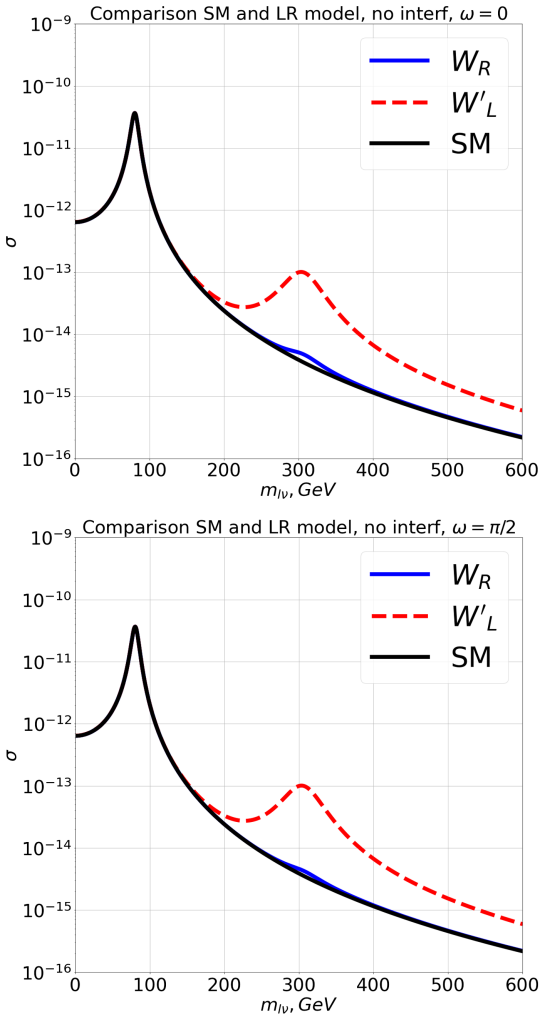


FIG. 17. Relative cross section of the W_R and W'_L production process at theoretical resonance widths: $\gamma_{W_L} = 10.7$ GeV, $\Gamma_{W_R} = 55$ GeV. The upper figure is for $\omega = 0$, the lower figure is for $\omega = \pi/2$.

out only based on its tail. The total count of events above an energy of 100 GeV is indicated by the black stepped line with experimental data points in Fig. 19. The same plot also shows a black normalization line for the Standard Model (SM) based on the tail of the left resonance. The white area below the black stepped line corresponds to the count of $e\nu$ events from the tail of the left resonance. Below that is a red area representing events involving the production of a top quark, followed by additional possible event types.

Our calculation results are presented on this plot for a resonance W' with a mass of 304 GeV as a red dashed line. Below it is a barely noticeable blue line, corresponding to the expected resonance with a mass of $M_{W_R} = 304$ GeV. It should be noted that in the resonance region, in addition to statistical errors from the left resonance, there are systematic errors associated with event identification, which are an order of magnitude larger. In this case, the statistics would have been sufficient to identify the resonance if it were not for the systematic errors of the experiment, which are an order of magnitude larger than the statistical errors.

The possibility of detecting right-handed currents in accelerator experiments was also discussed in work [58]. In it, the authors introduce the parameter ξ, which corresponds to the mixing angle ζ from the extended left-right model. According to formula (29) from [58], $|\xi_{ud}| < 0.04$ with 90% confidence, which can be compared to our result for the mixing angle $|\zeta| = 0.039 \pm 0.014$. The results are consistent with each other within 1.64σ.

Thus, in this section it was shown that the collider experiments do not contradict the results of our analysis about the

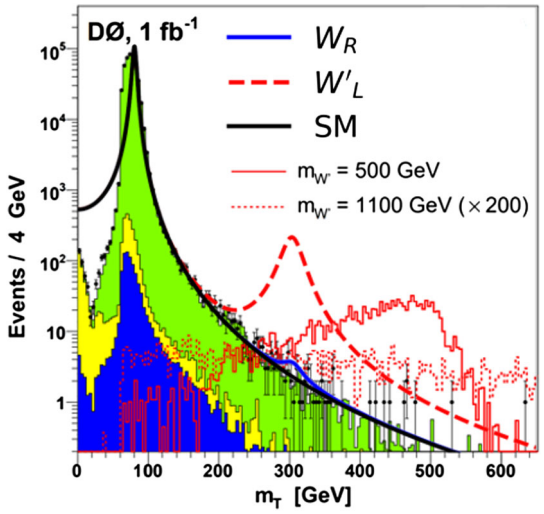


FIG. 18. The process of registration of the left vector boson at the Tevatron in Fermilab from the [56]. The resonance from the left vector boson is shown in green on the left. An example of the calculated signals for the resonance W'_L with masses 500 GeV and 1100 GeV are shown on the right. The results of our calculations are also shown here: (1) the black bold line shows the calculation according to the SM, (2) the dotted red line shows the resonance W'_L with a mass 304 GeV, (3) the bold blue line shows the expected resonance W_R with a mass $M_{W_R} = 304 \pm 24$ GeV.

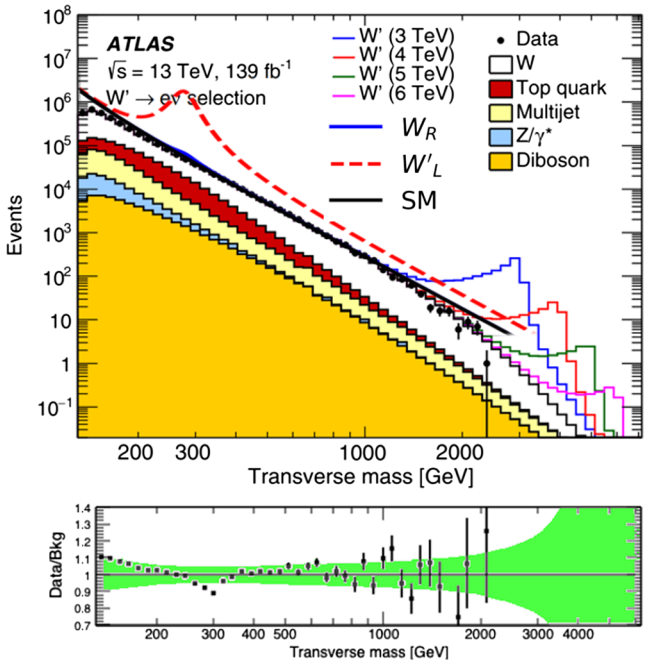


FIG. 19. Results of the ATLAS experiment [57]. The published results of the experiment are presented. The results of our calculations are also shown here: (1) the calculation according to the SM is shown by the black bold line, (2) the resonance W'_L with the mass 304 GeV is shown by the dotted red line, (3) the expected resonance W_R with the mass $M_{W_R} = 304 \pm 24$ GeV is shown by the bold, barely noticeable blue line. Systematic errors are indicated in green on the bottom panel.

possible existence of a right vector boson $M_{W_R} = 304^{+24}_{-20}$ GeV and a mixing angle with W_L: $\zeta = -0.039 \pm 0.014$.

VII. RESULTS OF DETERMINING THE MATRIX ELEMENT V_{ud} WITHIN THE LEFT-RIGHT MODEL OF $0^+ - 0^+$ TRANSITIONS AND NEUTRON DECAY

Now we should move on to the analysis of the situation with the superallowed Fermi $0^+ - 0^+$ transitions. These transitions occur due to the decay of W^+. In this process, the spin of the nucleus, equal to zero, and the positive parity of the nucleus are preserved, so this is a vector transition. The axial part is absent, and the parameter λ is not included in the definition of the quantity $(f\tau)^{00}$. It is this value that was carefully determined in the works J. C. Hardy and I. S. Towner [26]. They obtained average values $f\tau$ for each of the 21 transitions that have a complete dataset and then took into account the radiative and isospin corrections that break the symmetry. Fifteen of these values $f\tau$ have an accuracy of 0.3% or better, and all take the same value within the statistics, as expected from the conservation of vector current. Their average value, $f\tau$, combined with the muon lifetime, gives V_{ud} a quark mixing element of the CKM matrix of 0.97373 ± 0.00031. Thus, the value of the matrix element obtained within the V-A theory $V^{00}_{ud,SM} = 0.97373 \pm 0.00031$ and for neutron $V^{n}_{ud} = 0.97477(37)$ [27].

Using optimal parameter values $\lambda_{\text{opt}} = -1.2738 \pm 0.0012$, $\delta_{\text{opt}} = 0.070 \pm 0.010$, $\zeta_{\text{opt}} = -0.039 \pm 0.014$ and formulas (3.11), (3.16) we obtain values V_{ud} for $0^+ \to 0^+$ transitions and for neutron decay: $V^{00LR}_{ud} = 0.97346 \pm 0.00105$ $V^{nLR}_{ud} = 0.97661 \pm 0.00118$. These results are shown in Fig. 20.

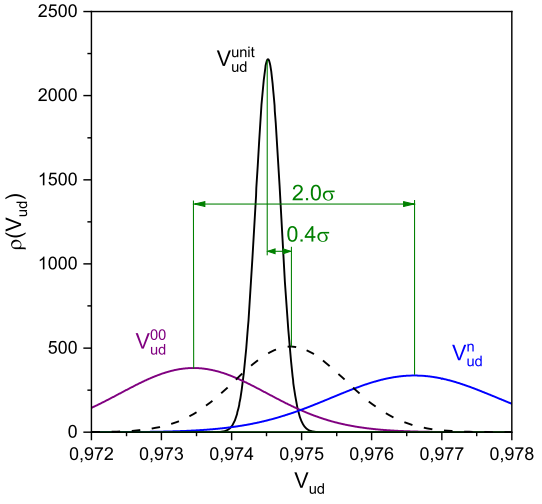


FIG. 20. Distribution for quantities V_{ud} for $0^+ \to 0^+$ transitions from neutron decay within the left-right model, as well as V_{ud} from the unitarity condition -$V^{\text{unit}}_{ud} = 0.97452 \pm 0.00018$.

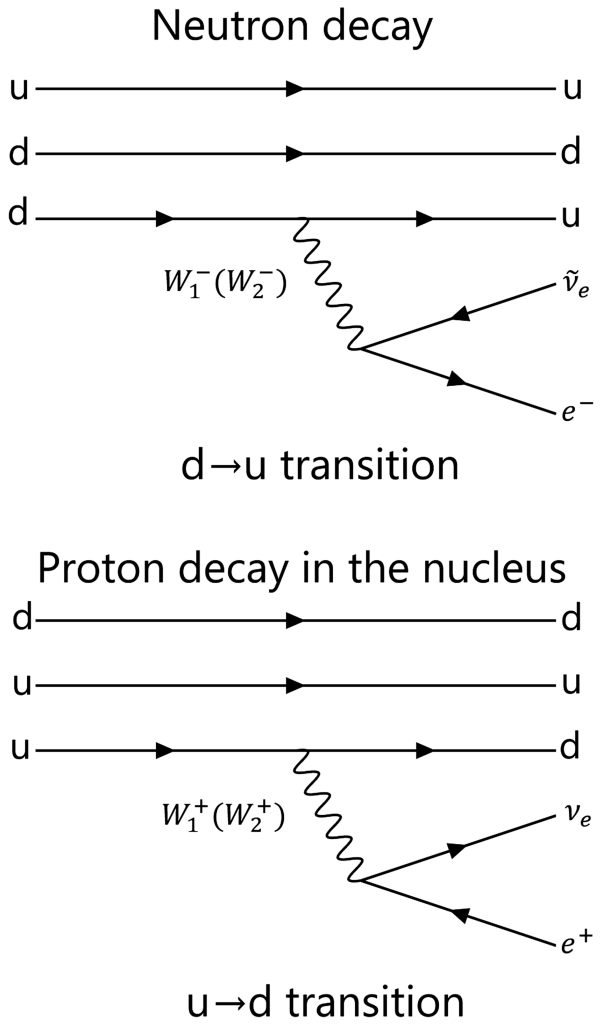


FIG. 21. The process of neutron decay and the process of proton decay in the nucleus. Direct transition from d-quark to u-quark and reverse transition from u-quark to d-quark.

Discrepancy between values V_{ud}^{00LR} and V_{ud}^{nLR} within the left-right model, is 2.0σ. A the deviation of their mean value from unitarity is 0.4σ. After considering the parameters of the left-right symmetric model, the difference between V_{ud}^{nLR} and V_{ud}^{00LR} increased by 3 times, but the error also increased by 3 times due to the errors δ, ζ and λ_{opt}. Therefore, the difference between V_{ud}^{nLR} and V_{ud}^{00LR} is 2.0σ.

It should be noted that the discrepancy between the values of V_{ud}^{00LR} and V_{ud}^{nLR} can be interpreted as a violation of CP invariance. since V_{ud}^{nLR} corresponds to the transition of the d quark to the u quark, and V_{ud}^{00LR} corresponds to the transition of the u quark to the d quark (Fig. 21). Note that the difference is that the neutron decay occurs via a negative vector boson in the mixed state $W_1^-(W_2^-)$, and the proton decays in the nucleus via a positive vector boson in the mixed state $W_1^+(W_2^+)$, and the sign of the mixing angle is opposite.

The CP violation parameter can be determined according to the Standard Model scheme, where to calculate the asymmetry, the probability of the process occurring via a positive vector boson is subtracted from the probability of the process occurring via a negative vector boson

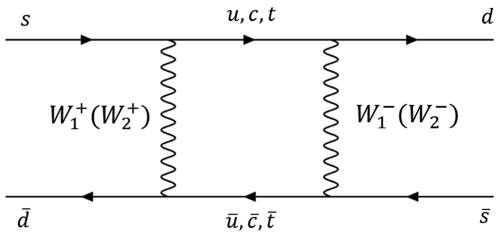
$$A_{p-n} = \frac{(V_{ud}^{00LR})^2 - (V_{ud}^{nLR})^2}{(V_{ud}^{00LR})^2 + (V_{ud}^{nLR})^2} = (-3.2 \pm 1.6) \times 10^{-3} (2.0\sigma) \tag{7.1}$$

Unfortunately, the accuracy of determining this parameter is still insufficient, but it is surprising that the value is in order of magnitude the values of the CP violation parameters in K-meson decays. However, the sign of asymmetry is opposite. Note that this is a baryon asymmetry that has not been observed experimentally before.

In this circumstance, it is useful to analyze the CP violation processes in K-meson decays within the framework of the extended left-right model, using the parameters δ and ζ.

VIII. ANALYSIS OF CP VIOLATION PROCESSES IN K-MESON DECAYS WITHIN THE EXTENDED LEFT-RIGHT MODEL USING THE PARAMETERS δ AND ζ

In the process of oscillations of the $K^0\overline{K}^0$ system, a decay into the state $e^-\pi^+\bar{\nu}$ or into the state $e^+\pi^-\nu$ can occur.



The weak interaction Hamiltonian with only vector currents can be represented in the same general form as for $0^+ \leftrightarrow 0^+$ transitions. However, K-mesons are pseudoscalar particles with zero spin and negative parity, so there are transitions $0^- \leftrightarrow 0^-$. Therefore, there is a ζ sign change compared to $0^+ \leftrightarrow 0^+$ transitions. For $0^- \leftrightarrow 0^-$ kaon-antikaon transitions we must write the Lagrangian with axial current:

$$H_V^N = \bar{e}\gamma_\mu (C_V + C'_V\gamma_5)\nu \cdot \bar{\pi}\gamma_\mu K^0, \tag{8.1}$$

where the decay of $W_1^-(W_2^-)$ is associated with the relation

$$|C_V|^2 + |C'_V|^2 = G_F^2 |V_{us}|^2 (1 + (\delta - \zeta)^2), \tag{8.2}$$

And decay of $W_1^+(W_2^+)$ associated with the relation

$$|C_V|^2 + |C'_V|^2 = G_F^2 |V_{us}|^2 (1 + (\delta + \zeta)^2) \tag{8.3}$$

The amplitude (8.1) can be written as [59]

$$M \simeq f_+(\bar{u}(3)\gamma_\mu(C_V + C'_V\gamma_5)\upsilon(2))p^\mu, \tag{8.4}$$

where f_+ = form factor, p = total momentum of pion and kaon, u = positron (electron), υ = neutrino (antineutrino)

$$M^*M \simeq |f_+|^2[u(3)\bar{u}(3)\gamma_\mu(C_V + C'_V\gamma_5) \times \upsilon(2)\bar{\upsilon}(2)\gamma^\sigma(C^*_V + C^*_V\gamma_5)]p^\mu p_\sigma \tag{8.5}$$

The probability of kaon decay is proportional to

$$\Gamma \propto |f_+|^2[|C_V|^2 + |C'_V|^2] \tag{8.6}$$

When decaying to the final state $e^+\pi^-\nu$ we have, up to quadratic terms,

$$\Gamma^{W^+} \propto |V_{us}|^2|f_+|^2[1 + (\delta + \zeta)^2] \tag{8.7}$$

When decaying into the final state $e^-\pi^+\bar{\nu}$, we have, up to quadratic terms,

$$\Gamma^{W^-} \propto |V_{us}|^2|f_+|^2[1 + (\delta - \zeta)^2] \tag{8.8}$$

Thus, taking into account (8.7) and (8.8), we obtain the formula for T-violating asymmetry:

$$A_T = \frac{\Gamma(\bar{K}^0 \to e^+\pi^-\nu) - \Gamma(K^0 \to e^-\pi^+\bar{\nu})}{\Gamma(\bar{K}^0 \to e^+\pi^-\nu) + \Gamma(K^0 \to e^-\pi^+\bar{\nu})} \tag{8.9}$$

which is equal to

$$A_T = \frac{1 + (\delta - \zeta)^2 - (1 + (\delta + \zeta)^2)}{2(1 + \delta^2 + \zeta^2)} \approx -2\delta\zeta \tag{8.10}$$

Using the previously obtained values $\delta = 0.070(10)$ and $\zeta = -0.039(14)$, we obtain the value for the

$$A_T^{LR} = (5.5 \pm 2.1) \times 10^{-3}(2.6\sigma) \tag{8.11}$$

This value is in absolute agreement with the experimentally measured asymmetry with available accuracy [60].

$$A_T^{\text{exp}} = (6.6 \pm 1.3 \pm 1.0) \times 10^{-3}(4\sigma) \tag{8.12}$$

Thus, the predictions of the extended left-right symmetric model are confirmed by the experiment with confidence level 2.6σ.

It is interesting to note that the experimental value of CP-violating asymmetry in the decay of neutral D mesons has a value quite close to the value of CP-violating asymmetry in the decay of neutral K mesons [61].

$$A_{D_0} = \frac{\Gamma(D_0 \to K^-K^+, \pi^-\pi^+) - \Gamma(\tilde{D}_0 \to K^-K^+, \pi^-\pi^+)}{2\Gamma}$$

$$A_{D_0}^{\text{exp}} = (6.30 \pm 0.33) \times 10^{-3}$$

As can be seen, the experimental values of CP-violating asymmetries are in good agreement. These are the so-called direct CP-violating effects, which arise during the oscillations of $K_0\bar{K}_0$ and $D_0\bar{D}_0$. The description of this effect within the framework of the left-right CP-violating model has already been presented for $K_0\bar{K}_0$. The procedure can be repeated in exactly the same way for $D_0\bar{D}_0$. In both cases, the effect of CP violation with mixing is described by the formula: $A_T^{LR} = -2\delta\zeta = (5.5 \pm 2.1) \times 10^{-3}(2.6\sigma)$ and gives the same result. Table III presents a comparison of the experimental results of direct CP-violating asymmetries and estimates within the framework of the left-right CP-violating model.

Besides, CP-violating lepton asymmetry A_L is measured more accurately in decays of neutral K-mesons with decay product detection in final state [60]

$$A_L = \frac{\Gamma(K_L \to e^+\pi^-\nu) - \Gamma(K_L \to e^-\pi^+\bar{\nu})}{\Gamma(K_L \to e^+\pi^-\nu) + \Gamma(K_L \to e^-\pi^+\bar{\nu})} \tag{8.13}$$

$$A_L^{\text{exp}} = (3.32 \pm 0.06) \times 10^{-3} \tag{8.14}$$

This asymmetry A_L^{exp} is two times smaller than A_T^{exp}. The fact is that the effect of CP violation with mixing is measured during the progress of the $K_0\bar{K}_0$ oscillation process over 10 periods of the lifetime of the K_S-state, which is 0.86×10^{-10} s. And the effect of CP violation in the final state is measured at the lifetimes of the K_L-state, which is 5.4×10^{-8} s. By this time, the effect associated with the K_S-state reduces. Therefore, $A_T/A_L = 2$ as shown in [60].

Of course, in our desire to understand the nature of CP violation, we must focus on the effect of CP violation with mixing. It determines the essence of the initial process. Its further development depends on a specific chain of decays. Therefore, within the framework of the model, we must explain only the main starting effect. It is surprising that this can be done using one simple relation $A_T^{LR} = -2\delta\zeta = (5.5 \pm 2.1) \times 10^{-3}(2.6\sigma)$. Of course, the confidence level does not give complete confidence, but it is at least higher than 99%.

TABLE III. Comparison of experimental results for CP-violating asymmetries with mixing for $K_0\bar{K}_0$ and $D_0\bar{D}_0$ and estimations within the framework of the left-right model in units of 10^{-3}.

	K^0	D^0
A^{exp}	6.6 ± 1.6	6.30 ± 0.33
A^{LR}	5.5 ± 2.1	5.5 ± 2.1

TABLE IV. Experimental results for *CP*-violating asymmetries in the final state in units of 10^{-3}.

	$p-n$	K_L^0
$A^{\exp}$	-3.2 ± 1.6	3.32 ± 0.06

Now let us consider to the *CP*-violating baryon asymmetry. The *CP*-violating baryon asymmetry from our comparison of V_{ud}^{nLR} and V_{ud}^{00LR} has an opposite sign.

$$A_{p-n} = \frac{(V_{ud}^{00LR})^2 - (V_{ud}^{nLR})^2}{(V_{ud}^{00LR})^2 + (V_{ud}^{nLR})^2} = (-3.2 \pm 1.6) \times 10^{-3} (2.0\sigma)$$

The opposite sign of the baryon asymmetry indicates that the B-L conservation condition, which was given in the famous work of A. D. Sakharov [62,63], is apparently satisfied.

The results for *CP*-violating asymmetries in the final state can be summarized in the following Table IV

Thus, we can summarize:

(1) There is agreement within the available accuracy between the experimental results of *CP*-violating asymmetries with mixing for the $K_0\bar{K}_0$ system and $D_0\bar{D}_0$ system and the estimations within the left-right model with the parameters obtained from neutron decay. The relation $A^{LR} = -2\delta\zeta$ is satisfied.

(2) There is agreement for absolute values within the available accuracy between the experimental results for *CP*-violating asymmetries in the final state for neutral K-mesons and *CP*-violating baryon asymmetry from our comparison V_{ud}^{nLR} and V_{ud}^{00LR} within the extended left-right model of the weak interaction with *CP* violation.

(3) Finally, it is very important to note that the signs of the baryon and lepton *CP*-violating asymmetries are different, which may be the reason for the conservation of the difference in the number of baryons and leptons during the formation of the Universe, B–L = const, $\Delta B = \Delta L$ [62,63].

IX. COMPARISON WITH THE RESULTS OF EXPERIMENTS WITH π-MESONS AND MUONS

In this section we explain why the TWIST experiment [64] is consistent with our analysis of neutron decay data.

In the TWIST experiment, fairly precise constraints on the mass of W_R and the mixing angle were obtained in the decay of the positive muon within the framework of the left-right manifest model: $-0.020 < \zeta < +0.017 (90\%\,\mathrm{CL})$ and $M_{W_R} > 592$ GeV$(90\%\,\mathrm{CL})$. The constraints on δ and ζ from the TWIST experiment are shown in Fig. 22 at the origin.

The description of the decays of π^+, π^- and μ^+, μ^- within the framework of the extended left-right model shows that, due to *CPT* conservation, the manifestation of

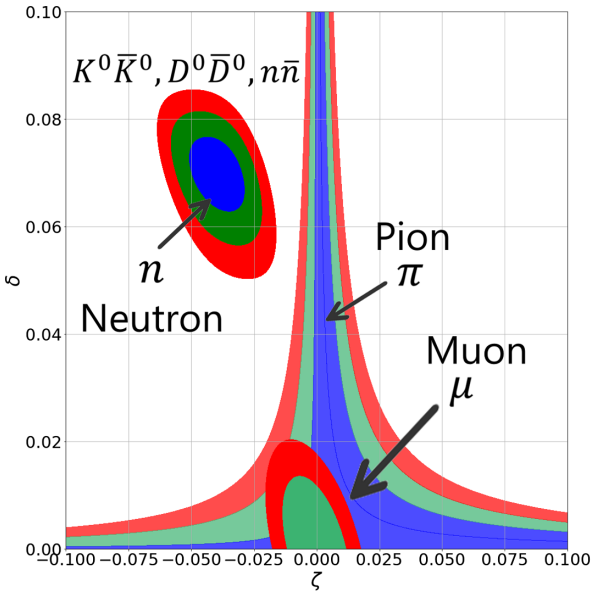


FIG. 22. Comparison of the results of the neutron decay analysis, which are also applicable to the decay asymmetries of $K^0\overline{K^0}$ and $D^0\overline{D^0}$, as well as constraints from *CPT* invariance for the decays $\pi^+\pi^-$ and $\mu^+\mu^-$. The asymmetry in the decays of charged particles, such as $\mu^\pm$ and $\pi^\pm$, is not possible, as shown on the graph.

CP violation is impossible for charged particles because of charge conservation, as well as *CPT* invariance. Indeed, for the π^+, π^- lifetime, one can write the already familiar relations for the amplitude of pion decay into two leptons:

$$M_{\pi^\pm \to \mu+\nu} \approx \left(\bar{\mu}\gamma_\rho \frac{(C_V^\pm + C_V'^\pm \gamma_5)}{2} \nu \right) \tag{9.1}$$

$C_V^\pm = 1 \pm 2\zeta + \delta$, $C_V'^\pm = 1 - \delta$ and for the ratio of the difference in lifetimes to the average lifetime we obtain

$$\frac{(\tau_{\pi^+} - \tau_{\pi^-})}{\tau_{\text{average}}} = -\frac{4\delta\zeta}{(1 + \delta^2 + \zeta^2)} \simeq -4\delta\zeta \tag{9.2}$$

However, this result implies a *CPT* violation, which in the decays π^+, π^-- is already has experimental constraints [65]. Such a process cannot be realized.

$$\frac{(\tau_{\pi^+} - \tau_{\pi^-})}{\tau_{\text{average}}} = (5.5 \pm 7.1) \times 10^{-4} \tag{9.3}$$

Even stronger constraints on *CPT* violation are available from decays K^0, $\bar{K}^0$ [66], where

$$\frac{(\Gamma_{K^0} - \Gamma_{\bar{K}^0})}{m_{\text{average}}} = (7.8 \pm 8.4) \times 10^{-18} \tag{9.4}$$

The manifestation of *CP*-invariance violation through the mixing of right-handed and left-handed W-bosons is only possible for neutral systems, such as $K^0 - \bar{K}^0$,

$D^0 - \bar{D}^0$, $B^0 - \bar{B}^0$, as well as for $n - \bar{n}$ oscillations. For these systems, the CPT theorem is not violated.

This is vividly demonstrated in the $K^0 - \overline{K^0}$ system, where the condition of equal masses for K^0 and $\overline{K^0}$ is satisfied with high precision.

Thus, the constraints for charged and neutral particles do not overlap, as shown in Fig. 22. The result of the TWIST experiment does not contradict the results of our analysis of neutron decay, nor the CP-violating effects in K^0 and D^0. These CP-violating effects for K^0 and D^0 can be described by the same parameters δ and ζ, extracted from neutron decay, as was shown in Sec. IV.

Thus, the extended version of the left-right model and the manifest model are not compatible.

X. BARYON-LEPTON ASYMMETRY OF THE UNIVERSE AND THE LEFT-RIGHT MODEL OF WEAK INTERACTION WITH *CP* VIOLATION

Now let us return to the question of the baryon-lepton asymmetry of the Universe and to the famous article by A. D. Sakharov [62,63]. This is a review report at a conference dedicated to the 100th anniversary of A.A. Friedman. Leningrad, June 22–26, 1988. This article formulates:

> "Three basic conditions for cosmological formation of baryonic asymmetry
> (I) Absence of baryonic charge conservation
> (II) Difference between particles and antiparticles, manifesting itself in the violation of CP-invariance.
> (III) Nonstationarity. Formation of BA is only possible under nonstationary conditions in the absence of local thermodynamic equilibrium."

In addition, the violation of both baryon and lepton asymmetry is discussed, and the conservation of the B-L difference is noted.

> "If the baryon-lepton asymmetry with $B \neq L$ arises at a temperature above the range $T = 10^2$–10^4 GeV… then a state will be established (with high precision) in the low temperature region which corresponds to the entropy maximum at given constant value of B—L = const (and under the condition of electric neutrality)."

Figure 23 shows the previously discussed dependence, which presents the difference B-L = const passing through 0 and through the equilibrium point, which, according to Sakharov s theorem, corresponds to the modern universe. Thus, all the main predictions of the baryon asymmetry of the Universe were made by A. D. Sakharov more than half a century ago, soon after the discovery of CP violation in K-mesons. Since then, the effects of CP violation have been thoroughly studied at accelerators, but the nature of CP violation has not been established. Although a method for describing CP violation through a complex phase in the CKM matrix has been proposed.

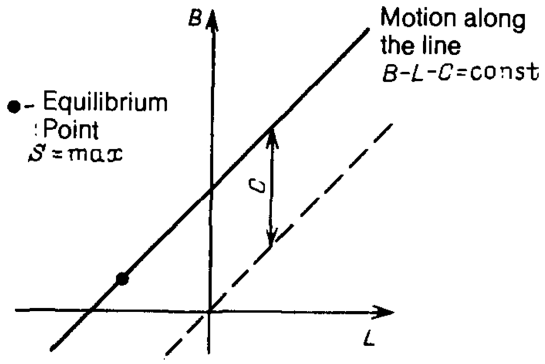


FIG. 23. A plot from A. D. Sakharov's paper, where the baryon and lepton asymmetries of the Universe are shown.

In our work, a left-right model of weak interaction with CP violation is proposed at mixing W_L and W_R, which indicates the nature of CP violation. In this regard, it is important to note that A. D. Sakharov's work speaks of the simultaneous formation of baryon and lepton asymmetry.

Now, based on the fact that the nature of CP violation is associated with the difference between left and right weak interactions, we can propose the following scenario for the formation of baryon and lepton asymmetry in the Universe.

At temperatures of the order of 10^4 GeV, the degree of symmetry between left and right processes (processes with opposite CP parity) was quite high. But when the temperature decreased, an advantage arose in preserving neutrons and protons in relation to antineutrons and antiprotons and simultaneously in preserving antineutrinos in relation to neutrinos.

Another important factor contributing to the generation of matter in the universe may be the asymmetry of neutron-antineutron oscillations due to CP violation. This violation can lead to a violation of the law of conservation of baryon number, which is necessary for Sakharov's first condition. Also, because neutrons and antineutrons decay by emitting different W bosons, the lifetime of the antineutron will differ from the neutron lifetime, which may also contribute to the generation of baryon asymmetry in the universe.

Therefore, proton accumulation occurs from neutron decay relative to antiprotons, leading to the formation of a positive baryon asymmetry of the universe. Simultaneously, there is an accumulation of antineutrinos, resulting in the formation of a negative lepton asymmetry of the universe.

Indeed, in the modern Universe we have protons and neutrons in nuclei, it is obvious that the baryon number is positive. Charged leptons are electrons in atoms, which indicates a positive asymmetry in the charged leptons sector, which is compensated excess of negative asymmetry due to a significant number of antineutrinos, therefore $L < 0$. If protons and neutrons formed galaxies, then neutrinos and antineutrinos formed dark matter located on the periphery of galaxies.

It is important to note that the existence of the W_R suggests the presence of right (so-called sterile) antineutrinos, which have a significantly greater mass than active neutrinos. They provide a mass of dark matter approximately 5 times greater than the mass of baryonic matter. The requirement for the stability of dark matter [1] and astrophysical observations [67] limit the mass of sterile neutrinos to below a few keV.

XI. POSSIBILITY OF INCREASING THE ACCURACY OF MEASUREMENTS IN NEUTRON DECAY

The left-right weak interaction model with CP violation presented here requires a significant increase in experimental precision.

There is a possibility of further increasing measurement accuracy in neutron decay. For example, this is the goal of the PNPI NRC KI project "Neutron Beta Decay" for the PIK reactor [68–70], which is planned to use a superconducting solenoid with a long flight base for neutron decay in order to increase the statistics of decay events and with a magnetic mirror-collimator to isolate the electron emission direction. It is a development of the PNPI RAS experiment of 1998 [22], and it is planned to achieve a relative measurement accuracy of 10^{-3} for neutrino and electron decay asymmetries, and most importantly, the asymmetries a and B, for which the greatest contradiction is now observed, will be measured with three times better accuracy.

Another project of the Technical University of Munich "PERC" for the FRM2 reactor [71] also uses a long superconducting solenoid with a magnetic mirror to measure neutrino and electron neutron decay asymmetries with a relative accuracy of $10^{-3}-10^{-4}$ [72]. Thus, there is reason to believe that the question of the existence W_R of with the above parameters will be clarified.

XII. CONCLUSION

(1) The results of the latest most accurate experimental data on neutron decay are presented. It has been shown that the accuracy of measurements has increased by more than an order of magnitude over the past 30 years, which allows for an analysis of inconsistencies of the Standard Model.

(2) An analysis was carried out on the possibility of the existence of the right vector boson W_R. As a result of the analysis within the framework of the extended left-right symmetric model, it was found that there is an indication of the existence of the right vector boson W_R with a mass $M_{W_R} = 304^{+24}_{-20}$ GeV, and a mixing angle with W_L: $\zeta = -0.039 \pm 0.014$.

(3) It is shown that this result does not contradict the experiments at colliders to search for a hypothetical vector boson.

(4) CP violation was found in the baryon sector at the 2σ confidence level.

(5) It is shown that it is possible to describe the effects of CP violation in decays of neutral K-mesons and D-mesons using the parameters of the extended left-right model, which are obtained from neutron decay.

Thus, the extended left-right symmetric model of weak interaction within the limits of the available accuracy, allows to describe the effects of CP violation in baryons and mesons using relation $A^{LR} = -2\delta\zeta$.

(6) The opposite signs of the baryon and lepton CP-violating asymmetry are associated with the different signs of the baryon and lepton asymmetry of the Universe, and B-L is conserved [62,63].

(7) Finally, we can consider possible consequences, assuming the results presented in this work will be confirmed. First, an extension of SM by introducing right vector bosons $W_R^{\pm}, Z_R$ and righthanded neutrinos is required. Second, righthanded neutrinos can be considered as candidates for dark matter.

ACKNOWLEDGMENTS

The authors express their gratitude to the staff of the High Energy Physics Department of PNPI for assistance in analyzing the ATLAS experiment data. This work was supported by the Russian Science Foundation (Project No. 24-12-00091) [73].

The authors declare no conflict of interest.

[1] A. P. Serebrov, R. M. Samoilov, O. M. Zherebtsov, and N. S. Budanov, Proc. Sci., ICPPCRubakov2023 (**2024**) 044.
[2] A. P. Serebrov, R. M. Samoilov, O. M. Zherebtsov, and N. S. Budanov, arXiv:2306.09962v2.
[3] M. A. B. Beg, R. V. Budny, R. Mohapatra, and A. Sirlin, Phys. Rev. Lett. **38**, 1252 (1977).
[4] Barry R. Holstein and S. B. Treiman, Phys. Rev. D **16**, 2369 (1977).
[5] P. Herczeg, Phys. Rev. D **34**, 3449 (1986).
[6] P. Herczeg, Prog. Part. Nucl. Phys. **46**, 413 (2001).
[7] N. Severijns, M. Beck, and O. Naviliat-Cuncic, Rev. Mod. Phys. **78**, 991 (2006)].

[8] A. P. Serebrov, V. E. Varlamov, A. G. Kharitonov *et al.*, Phys. Lett. B **605**, 72 (2005).
[9] V. Ezhov, *Proceedings of "The Seventh UCN Workshop". 2009. St. Petersburg, Russia (2009)* http://cns.pnpi.spb.ru/7UCN/articles/Ezhov1.pdf.
[10] V. F. Ezhov, A. Z. Andreev, G. Ban *et al.*, JETP Lett. **107**, 671 (2018).
[11] R. W. Pattie Jr., N. B. Callahan, C. Cude-Woods *et al.*, Science **360**, 627 (2018).
[12] F. M. Gonzalez, E. M. Fries, C. Cude-Woods *et al.*, Phys. Rev. Lett. **127**, 162501 (2021).
[13] A P Serebrov, Phys. Usp. **62**, 596 (2019).
[14] S. Arzumanov, L. Bondarenko, S. Chernyavsky *et al.*, Phys. Lett. B **483**, 15 (2000).
[15] Y. Fuwa, T. Hasegawa, K. Hirota *et al.*, arXiv:2412.19519v1.
[16] S. Navas *et al.* (Particle Data Group), Phys. Rev. D **110**, 030001 (2024).
[17] F. E. Wietfeldt, W. A. Byron, B. Collett, M. S. Dewey, T. R. Gentile, F. Gluck, M. T. Hassan, G. L. Jones, A. Komives, J. S. Nico, and E. J. Stephenson, Phys. Rev. C **110**, 015502 (2024).
[18] M. Beck, W. Heil, C. Schmidt, S. Baessler, F. Gluck, G. Konrad, and U. Schmidt, Phys. Rev. Lett. **132**, 102501 (2024).
[19] D. Mund, B. Märkisch, M. Deissenroth, J. Krempel, M. Schumann, H. Abele, A. Petoukhov, and T. Soldner, Phys. Rev. Lett. **110**, 172502 (2013).
[20] B. Märkisch *et al.*, Phys. Rev. Lett. **122**, 242501 (2019).
[21] B. Märkisch, CKM2023. https://indico.cern.ch/event/1184945/contributions/5540848/attachments/2719237/4723864/Maerkisch%20CKM%202023%20-1.pdf.
[22] A. P. Serebrov *et al.*, J. Exp. Theor. Phys. **86**, 1074 (1998).
[23] M. Schumann *et al.*, Phys. Rev. Lett. **99**, 191803 (2007).
[24] M. Beck, F. Ayala Guardia, M. Borg *et al.*, Phys. Rev. C **101**, 055506 (2020).
[25] J. C. Hardy and I. S. Towner, Phys. Rev. C **91**, 025501 (2015).
[26] J. C. Hardy and I. S. Towner, Phys. Rev. C **102**, 045501 (2020).
[27] A. Czarnecki, William J. Marciano, and A. Sirlin, Phys. Rev. D **100**, 073008 (2019).
[28] A. Falkowski, M. González-Alonso, O. Naviliat-Cuncic, and N. Severijns, Eur. Phys. J. A **59**, 113 (2023).
[29] A. N. Ivanov, M. Pitschmann, and N. I. Troitskaya, Phys. Rev. D **88**, 073002 (2013).
[30] I. A. Kuznetsov, A. P. Serebrov, I. V. Stepanenko, A. V. Alduschenkov, M. S. Lasakov, A. A. Kokin, Y. A. Mostovoi, B. G. Yerozolimsky, and M. S. Dewey, Phys. Rev. Lett. **75**, 794 (1995).
[31] Chien-Yeah Seng, Phys. Rev. C **109**, 035501 (2024).
[32] R. Musedinovic *et al.*, Phys. Rev. C **111**, 045501 (2025).
[33] A. Sirlin, Rev. Mod. Phys. **50**, 573 (1978).
[34] W. J. Marciano and A. Sirlin, Phys. Rev. Lett. **56**, 22 (1986).
[35] William J. Marciano and A. Sirlin, Phys. Rev. Lett. **96**, 032002 (2006).
[36] A. Czarnecki, William J. Marciano, and A. Sirlin, Phys. Rev. D **70**, 093006 (2004).
[37] Vincenzo Cirigliano, Wouter Dekens, Emanuele Mereghetti, and Oleksandr Tomalak, Phys. Rev. D **108**, 053003 (2023).
[38] D. H. Wilkinson, Nucl. Phys. **A377**, 474 (1982).
[39] V. Cirigliano, A. Crivellin, M. Hoferichter, and M. Moulson, Phys. Lett. B **838**, 137748 (2023).
[40] Chien-Yeah Seng, Mikhail Gorchtein, Hiren H. Patel, and Michael J. Ramsey-Musolf, Phys. Rev. Lett. **121**, 241804 (2018).
[41] Chien-Yeah Seng, Mikhail Gorchtein, and Michael J. Ramsey-Musolf, Phys. Rev. D **100**, 013001 (2019).
[42] K. Shiells, P. G. Blunden, and W. Melnitchouk, Phys. Rev. D **104**, 033003 (2021).
[43] Peng X. Ma, X. Feng, M. Gorchtein, Lu C. Jin, Keh F. Liu, Chien Y. Seng, Bi G. Wang, and Zhao L Zhang,. Phys. Rev. Lett. **132**, 191901 (2024).
[44] F. Glück, Phys. Rev. D **47**, 2840 (1993).
[45] F. Gluck, Phys. Lett. B **436**, 25 (1998).
[46] A. P. Serebrov, O. M. Zherebtsov, A. K. Fomin, R. M. Samoylov, and N. S. Budanov, Phys. Part. Nucl. Lett. **22**, 229 (2025).
[47] V. Gudkov, K. Kubodera, and F. Myhrer, J. Res. Natl. Inst. Stand. Technol. **110**, 315 (2005).
[48] J. David Bowman *et al.*, arXiv:1410.5311v1.
[49] Gertrud Konrad and Hartmut Abele, Proc. Sci., INPC2016 (**2016**) 359.
[50] G. Darius *et al.*, Phys. Rev. Lett. **119**, 042502 (2017).
[51] Dirk Dubbers and Bastian Märkisch, Annu. Rev. Nucl. Part. Sci. **71**, 139 (2021).
[52] G. Bison *et al.*, Phys. Rev. C **95**, 045503 (2017).
[53] A. Kozela *et al.*, J. Phys. Conf. Ser. **2586**, 012139 (2023).
[54] E. Boos, V. Bunichev, L. Dudko, and M. Perfilov, Phys. Lett. B **655**, 245 (2007).
[55] F. E. Wietfeldt, W. A. Byron, B. Collet *et al.*, Phys. Rev. C **110**, 015502 (2024).
[56] V. M. Abazov *et al.* (D0 Collaboration), Phys. Rev. Lett. **100**, 031804 (2008).
[57] G. Aad *et al.* (ATLAS Collaboration), Phys. Rev. D **100**, 052013 (2019).
[58] S. Alioli, V. Cirigliano, W. Dekens, J. de Vries, and E. Mereghetti, J. High Energy Phys. 05 (2017) 086.
[59] L. B. Okun, *Leptons and Quarks (Special Edition Commemorating the Discovery of the Higgs Boson)* (World Scientific, Singapore, 2014), 10.1142/9162.
[60] A. Angelopoulos *et al.* (CPLEAR Collab), Eur. Phys. J. C **22**, 55 (2001).
[61] LHCb Collaboration, J. High Energy Phys. 12 (2021) 141.
[62] A. D. Sakharov, JETP Lett. **5**, 24 (1967).
[63] A. D. Sakharov, Sov. Phys. Usp. **34**, 417 (1991).
[64] J. F. Bueno, R. Bayes, Yu. I. Davydov *et al.*, Phys. Rev. D **84**, 032005 (2011).
[65] D. S Ayres *et al.*, Phys. Rev. D **3**, 1051 (1971).
[66] A. Angelopoulos *et al.*, Phys. Lett. B **471**, 332 (1999).
[67] Brandon M. Roach, S. Rossland, C. Y. Ng Kenny, K. Perez, John F. Beacom, Brian W. Grefenstette, S. Horiuchi, R. Krivonos, and Daniel R. Wik, Phys. Rev. D **107**, 023009 (2023).

[68] O. B. Belomytsev, A. V. Vasiliev, Yu. P. Rudnev, and A. P. Serebrov, preprint LNPI—1391 (1988).
[69] A. Serebrov, Yu. Rudnev, A. Murashkin *et al.*, J. Res. Natl. Inst. Stand. Technol. **110**, 383 (2005).
[70] A. P. Serebrov, Yu. P. Rudnev, A. N. Murashkin *et al.*, Nucl. Instrum. Methods **545**, 344 (2005).
[71] D. Dubbers, Nucl. Instrum. Methods Phys. Res., Sect. A **596**, 238 (2008).
[72] B. Märkisch, EXA2017 https://indico.gsi.de/event/5012/contributions/23286/attachments/17026/21492/exa2017_maerkisch_170914.pdf.https://rscf.ru/project/24-12-00091/.
[73] https://rscf.ru/project/24-12-00091/.